

Fabrication of two-dimensional van der Waals moiré superlattices

Zihao Wan(万子豪), Chao Wang(王超), Hang Zheng(郑航), Wenna Tang(唐文娜), Zihao Fu(付梓豪), Weilin Liu(刘伟林), Zhenjia Zhou(周振佳), Jun Li(李骏), Guowen Yuan(袁国文), and Libo Gao(高力波)

Citation: Chin. Phys. B, 2025, 34 (**4**): 047302. DOI: 10.1088/1674-1056/adb38b
Journal homepage: http://cpb.iphy.ac.cn; http://iopscience.iop.org/cpb

What follows is a list of articles you may be interested in

Emergence of metal-semiconductor phase transition in MX_2(M = Ni, Pd, Pt; X = S, Se, Te) moiré superlattices

Jie Li(李杰), Rui-Zi Zhang(张瑞梓), Jinbo Pan(潘金波), Ping Chen(陈平), and Shixuan Du(杜世萱)
Chin. Phys. B, 2025, 34 (**3**): 037302. DOI: 10.1088/1674-1056/ada7d9

Phase changings in the surface layers of T_d-WTe_2 driven by alkali-metal deposition

Yu Zhu(朱玉), Zheng-Guo Wang(王政国), Yu-Jing Ren(任宇靖), Peng-Hao Yuan(袁鹏浩), Jing-Zhi Chen(陈景芝), Yi Ou(欧仪), Li-Li Meng(孟丽丽), and Yan Zhang(张焱)
Chin. Phys. B, 2025, 34 (**1**): 017302. DOI: 10.1088/1674-1056/ad9e9e

A universal resist-assisted metal transfer method for 2D semiconductor contacts

Xuanye Liu(刘轩冶), Linxuan Li(李林璇), Chijun Wei(尉驰俊), Peng Song(宋鹏), Hui Gao(高辉), Kang Wu(吴康), Nuertai Jiazila(努尔泰·加孜拉), Jiequn Sun(孙杰群), Hui Guo(郭辉), Haitao Yang(杨海涛), Wu Zhou(周武), Lihong Bao(鲍丽宏), and Hong-Jun Gao(高鸿钧)
Chin. Phys. B, 2024, 33 (**12**): 127302. DOI: 10.1088/1674-1056/ad8db4

Anomalous valley Hall effect in two-dimensional valleytronic materials

Hongxin Chen(陈洪欣), Xiaobo Yuan(原晓波), and Junfeng Ren(任俊峰)
Chin. Phys. B, 2024, 33 (**4**): 047304. DOI: 10.1088/1674-1056/ad1c59

InSe-Te van der Waals heterostructures for current rectification and photodetection

Hao Wang(王昊), Guo-Yu Xian(冼国裕), Li Liu(刘丽), Xuan-Ye Liu(刘轩冶), Hui Guo(郭辉), Li-Hong Bao(鲍丽宏), Hai-Tao Yang(杨海涛), and Hong-Jun Gao(高鸿钧)
Chin. Phys. B, 2023, 32 (**8**): 087303. DOI: 10.1088/1674-1056/acd2b1

TOPICAL REVIEW — Moiré physics in two-dimensional materials

Fabrication of two-dimensional van der Waals moiré superlattices

Zihao Wan(万子豪), Chao Wang(王超), Hang Zheng(郑航), Wenna Tang(唐文娜), Zihao Fu(付梓豪), Weilin Liu(刘伟林), Zhenjia Zhou(周振佳), Jun Li(李骏), Guowen Yuan(袁国文)†, and Libo Gao(高力波)‡

National Laboratory of Solid State Microstructures, Jiangsu Key Laboratory for Nanotechnology, School of Physics, Collaborative Innovation Center of Advanced Microstructures, Nanjing University, Nanjing 210093, *China*

(Received 26 October 2024; revised manuscript received 3 January 2025; accepted manuscript online 7 February 2025)

Two-dimensional (2D) van der Waals (vdW) moiré superlattices have attracted significant attention due to their novel physical properties and quantum phenomena. The realization of these fascinating properties, however heavily depends on the quality of the measured moiré superlattices, emphasizing the importance of advanced fabrication techniques. This review provides an in-depth discussion of the methods for fabricating moiré superlattices. It begins with a brief overview of the structure, properties, and potential applications of moiré superlattices, followed by a detailed examination of fabrication techniques, focuses on different kinds of transfer techniques and growth methods, particularly chemical vapor deposition (CVD) method. Finally, it addresses current challenges in fabricating high-quality moiré superlattices and discusses potential directions for future advancements in this field. This review will enhance the understanding of moiré superlattice fabrication and contributing to the continued development of 2D twistronics.

Keywords: 2D materials, moiré superlattices, fabrication techniques, chemical vapor deposition (CVD)

PACS: 73.40.Lq, 81.15.Gh, 82.45.Mp

DOI: 10.1088/1674-1056/adb38b **CSTR:** 32038.14.CPB.adb38b

1. Introduction

Since the pioneering work of Novoselov and Geim in 2004, who isolated monolayer graphene using mechanical exfoliation,[1] the field of two-dimensional (2D) materials has attracted significant research interest. A variety of 2D materials have been identified, including transition metal dichalcogenides (TMDCs),[2–6] hexagonal boron nitride (hBN),[7–11] black phosphorus (BP),[12–16] 2D transition metal carbides or nitrides (MXenes),[17–21] etc. The ultra-thin nature of these materials results in their physical properties being sensitive to external conditions, such as magnetic field, electric field, and strain, particularly at low temperature and under strong magnetic conditions. This sensitivity of 2D materials allows for a range of tunable physical properties, underscoring the versatility of 2D materials. Furthermore, the weak van der Waals (vdW) interactions among 2D materials facilitate the stacking of these materials into heterostructures without the need of lattice matching.[22] This modular approach resembles constructing with Lego bricks, where carefully chosen functional materials serve as building blocks, enabling the engineered design of novel systems with emergent properties rather than mere additive effects.[23]

In addition to constructing novel 2D systems with vdW heterostructures, moiré superlattices can be engineered by exploiting the interlayer twist angle as an additional parameter. These superlattices are obtained by capitalizing the interfacial angles or lattice mismatches of the stacked 2D materials to create moiré patterns and result in new long-range periodic superlattice structures, as shown in Figs. 1(a) and 1(b). The year 2018 marked a significant milestone in moiré superlattice research, as Cao *et al.* successfully fabricated twisted bilayer graphene (TBG) moiré superlattices at the "magic angle" of 1.1° using the tear-and-rotate method.[24] This breakthrough leads to the observation of a plethora of fascinating physical phenomena, including the strong correlation effect,[25] the quantum anomalous Hall effect,[26] the fractional quantum anomalous Hall effect,[27,28] unconventional superconductivity,[24] ferromagnetism,[29] moiré exciton,[30] ferroelectricity,[31] and Wigner crystal.[32] The field of twistronics is burgeoning, as depicted in Fig. 1(c).

Despite the rich physical properties of moiré superlattices, their measurement is highly contingent on the quality of the crystal structures. Consequently, each novel physical phenomenon has inspired researchers to investigate more advanced fabrication techniques for these structures. With continuous improvements in the fabrication methods for 2D materials, the technology for creating moiré superlattices is also maturing and evolving, facilitating their developments. The evolution of fabrication technology is shown in Fig. 1(d). The methods for preparing moiré superlattices are becoming increasingly diverse, with ongoing enhancements in both the quality and size. It is anticipated that the fabrication of moiré superlattices will achieve mass production and commercial development in the near future, and provide a reliable platform for the exploration of moiré physics.

†Corresponding author. E-mail: gwyuan@nju.edu.cn

‡Corresponding author. E-mail: lbgao@nju.edu.cn

© 2025 Chinese Physical Society and IOP Publishing Ltd. All rights, including for text and data mining, AI training, and similar technologies, are reserved.

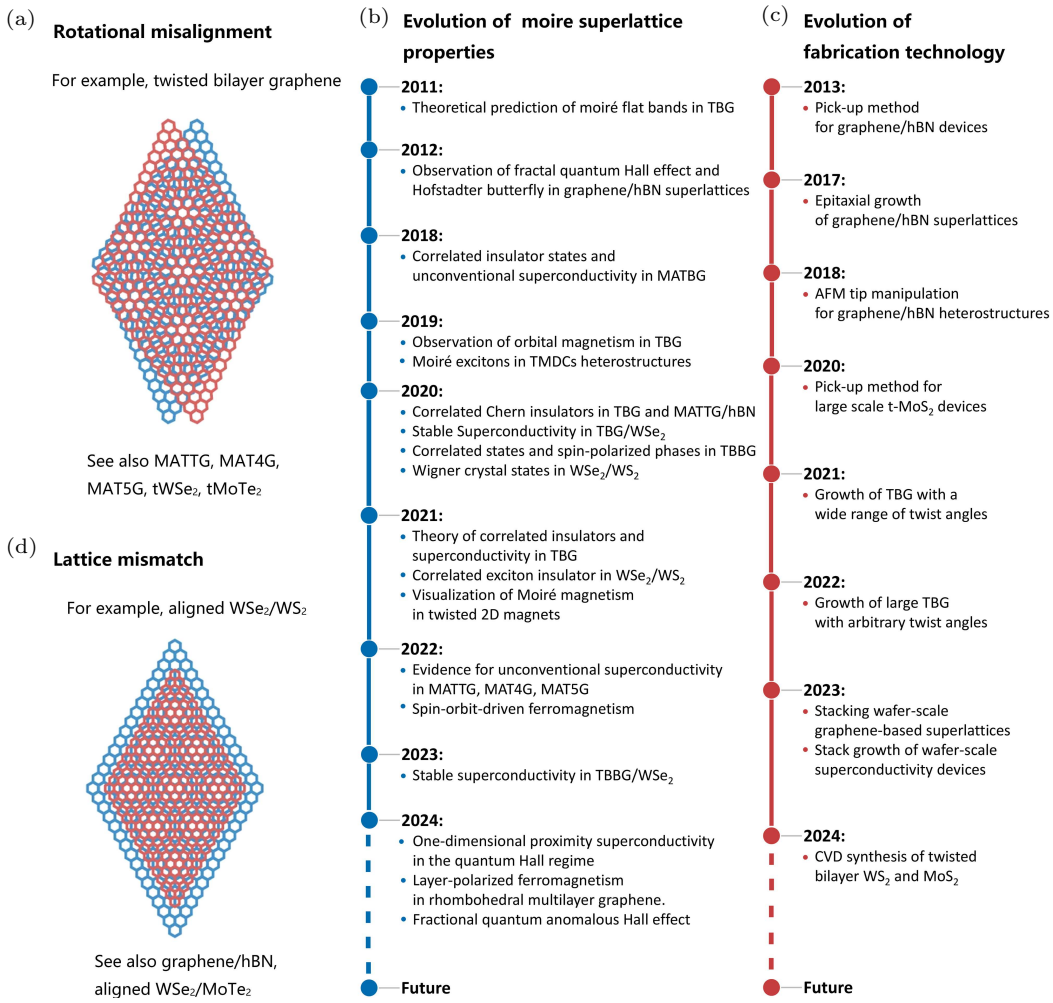


Fig. 1. Moiré pattern and evolution of moiré superlattices. Schematic of moiré patterns induced by interlayer twist angles (a) and lattice misalignment (b). Reproduced with permission from Ref. [33]. (c) Timeline of discoveries regarding the physical properties of moiré superlattices. (d) Evolution of fabrication methods for moiré superlattices.

In this review, we begin with an overview of the structures of moiré superlattices, followed by a systematic introduction of the fabrication methods employed for moiré superlattices, including transfer techniques and growth methods. In particular, we provide a detailed discussion of the chemical vapor deposition (CVD) growth method due to its unique advantages in the preparation of wafer-scale, high-quality, ultra-uniform moiré superlattices. Finally, we outline the challenges inherent in the fabrication process and propose some potential solutions to address these challenges.

2. The 2D moiré superlattices

In twisted moiré superlattice systems, the emergence of moiré patterns is primarily attributed to the interlayer twist angles between 2D materials. The characteristics of these moiré patterns in superlattices vary with different twist angles.[34] In 2011, MacDonald and Bistritzer theorized that at a critical angle of 1.05°, these layers form moiré superlattices with flat bands.[35] The first experimental realization of this "magic-angle" twisted bilayer graphene (MATBG) moiré superlattice device was achieved by Cao *et al.* in 2018,[24] as shown in Fig. 2(a). Subsequently, Wang's research group successfully observed and visualized the flat band structure in MATBG using angle-resolved photoemission spectroscopy (ARPES) technology.[36]

In the 2D moiré superlattices system with small twist angles, the moiré patterns are modulated by the atomic reconstruction that arises from vdW interlayer interactions.[37] The dark-field image of a slightly twisted TBG sample at 0.1° reveals a pattern of triangular shapes that switch between two types of symmetry (AB and BA), aligning with the repeating moiré pattern,[38] as shown in Fig. 2(b). This observation indicates the presence of interfacial atomic reconstruction in TBG. As the angle increases, the clear pattern of the triangle fades, and transitions into straight lines oriented in one direction, which usually appear in simple twisted moiré superlattices devoid of reconstruction.[39] Moreover, atomic reconstruction substantially contributes to the moiré patterning in twisted bilayer hBN, resulting in a lattice-relaxed arrangement characterized by alternating triangular AB/BA domains, which also induces out-of-plane polarization due to the electric dipole moment.[40] However, in TMDCs systems, it is generally easy to form near-R-stacked and near-H-stacked moiré superlattices, as shown in Fig. 2(e).[41]

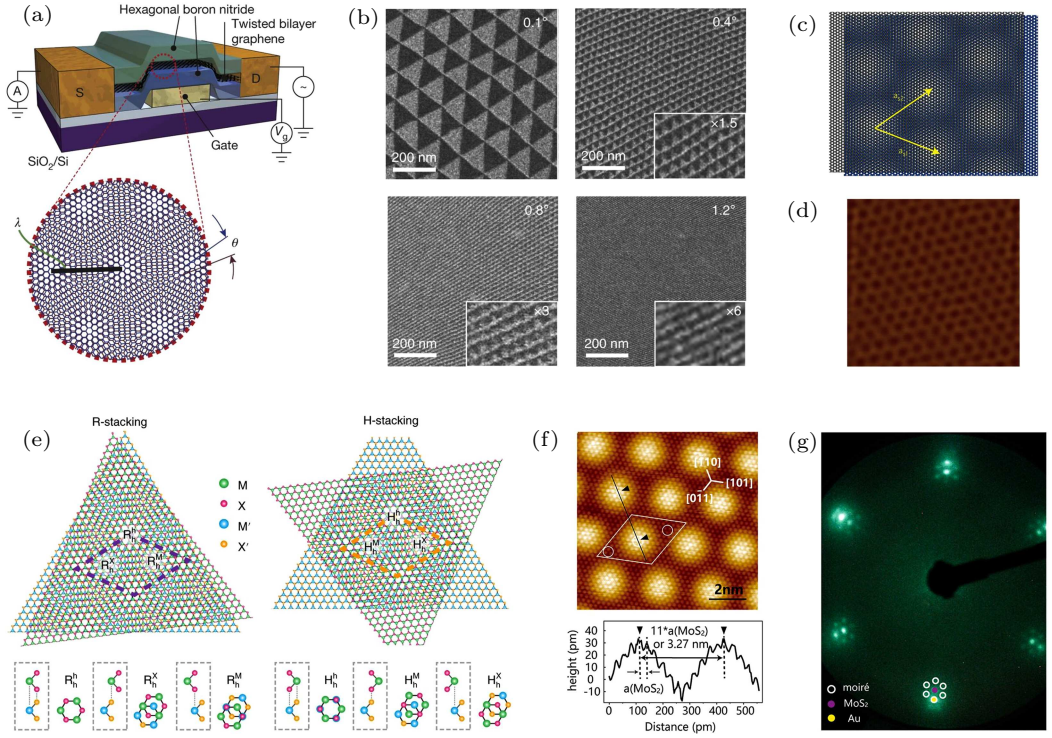


Fig. 2. Structures of moiré superlattices. (a) Schematic diagram of a MATBG device. Reproduced with permission from Ref. [25]. (b) Transmission electron microscope (TEM) dark-field images of TBG with a series of controlled twist angles. Reproduced with permission from Ref. [38]. A schematic illustration (c) and a scanning tunneling microscope (STM) image (d) of graphene/hBN moiré superlattices with zero rotation angle. Reproduced with permission from Ref. [42]. (e) Near-R-stacked and near-H-stacked moiré superlattices. Reproduced with permission from Ref. [41]. STM image (f) and low energy electron diffraction (LEED) pattern (g) of the MoS_2/Au(111) moiré superlattice. Reproduced with permission from Ref. [43].

In addition to twist-induced moiré superlattices, the lattice mismatch between disparate 2D materials can also result in the formation of moiré superlattices.[44] Yang *et al.* identified moiré patterns in graphene/hBN heterostructures with a twist angle of zero degrees,[42] as shown in Figs. 2(c) and 2(d). Moreover, Bao *et al.* grew MoS_2 on Au(111), resulting in a MoS_2/Au moiré superlattice with a moiré period of 3.27 nm,[43] as shown in Figs. 2(f) and 2(g). Furthermore, an increasing number of moiré superlattices are being discovered, such as magic-angle twisted trilayer graphene (MATTG), twisted bilayer-bilayer graphene (TBBG), twisted monolayer bilayer graphene (TMBG), magic-angle twisted quadrilayer graphene (MAT4G), magic-angle twisted pentalayer graphene (MAT5G), and these emerging moiré superlattices provide a reliable platform for the study of moiré physical properties.[45–48]

The periodicity of moiré patterns is significantly influenced by both the relative orientation angle and lattice mismatch between the 2D material layers, and can be quantitatively described by the mathematical formula[49]

$$\lambda = \frac{(1+\delta)a}{\sqrt{2(1+\delta)(1-\cos\theta)+\delta^2}},$$

where λ is the moiré pattern period of the moiré superlattice, δ is the lattice mismatch size between different materials, a is the lattice constant, and θ is the relative angle of rotation.

3. Fabrication of moiré superlattices

Moiré superlattices exhibit a large number of exotic quantum phenomena, making them an important platform for investigating low-dimensional physics. Moreover, moiré superlattices hold vast and crucial potential for future applications. Consequently, achieving controlled fabrication of moiré superlattices is essential for harnessing their potential. Moiré superlattices can be produced through various methods, primarily including transfer techniques and growth methods, which enable researchers to modify their properties for specific applications.

3.1. Stack transfer

3.1.1. Mechanical exfoliation and stack transfer techniques

Mechanical exfoliation and stack transfer are a well-established technique for fabricating moiré superlattices. Over time, this fabrication method has evolved and become more sophisticated, maintaining its status as an indispensable tool for scientists in the exploration of fundamental physics.

In 2010, Dean *et al.* fabricated graphene/hBN heterostructures using mechanical transfer method.[50] Firstly, they exfoliated graphene onto a SiO_2/Si substrate with a surface composed of a water-soluble layer and polymethyl methacrylate (PMMA). Then, they immersed the substrate with the exfoliated graphene into a water solution, and as the

water-soluble layer dissolved, the graphene/PMMA floated on the water surface. Next, they used a glass slide to pick up the graphene/PMMA and then proceeded to dry it. After drying, they transferred the graphene onto the prepared hBN/SiO_2/Si substrate, as shown in Fig. 3(a). Due to the absence of hanging bonds on the hBN surface and the atomic-level flatness, the graphene in the graphene/hBN heterostructures exhibits high mobility. However, this transfer process inevitably leaves residual adhesive at the superlattice interface, which can still impact the intrinsic physical properties of the 2D materials.

To solve this problem, Wang *et al.* developed a "pick-up" dry transfer method for fabricating superlattices in 2013, which features an extremely clean atomic-level interface, thereby allowing 2D materials to display their inherent physical properties.[51] Firstly, they used poly-propylene carbonate (PPC) to exfoliate hBN, then placed the hBN/PPC on a polydimethylsiloxane (PDMS) substrate with the hBN facing outward. Next, they aligned the hBN/PPC/PDMS with the pre-exfoliated graphene, and picked up the graphene onto the hBN, forming a graphene/hBN/PPC/PDMS structure. Afterward, the graphene/hBN/PPC/PDMS structure is placed over the pre-exfoliated hBN on a SiO_2/Si substrate, creating an hBN/graphene/hBN/PPC/PDMS structure. Finally, the PDMS and PPC were removed, yielding an hBN/graphene/hBN heterostructure, as illustrated in Fig. 3(b). The pick-up dry transfer method, which fabricates heterostructures with very high quality, can be extended to the fabrication of superlattices from nearly all exfoliated 2D materials, with virtually no limit on the number of layers.

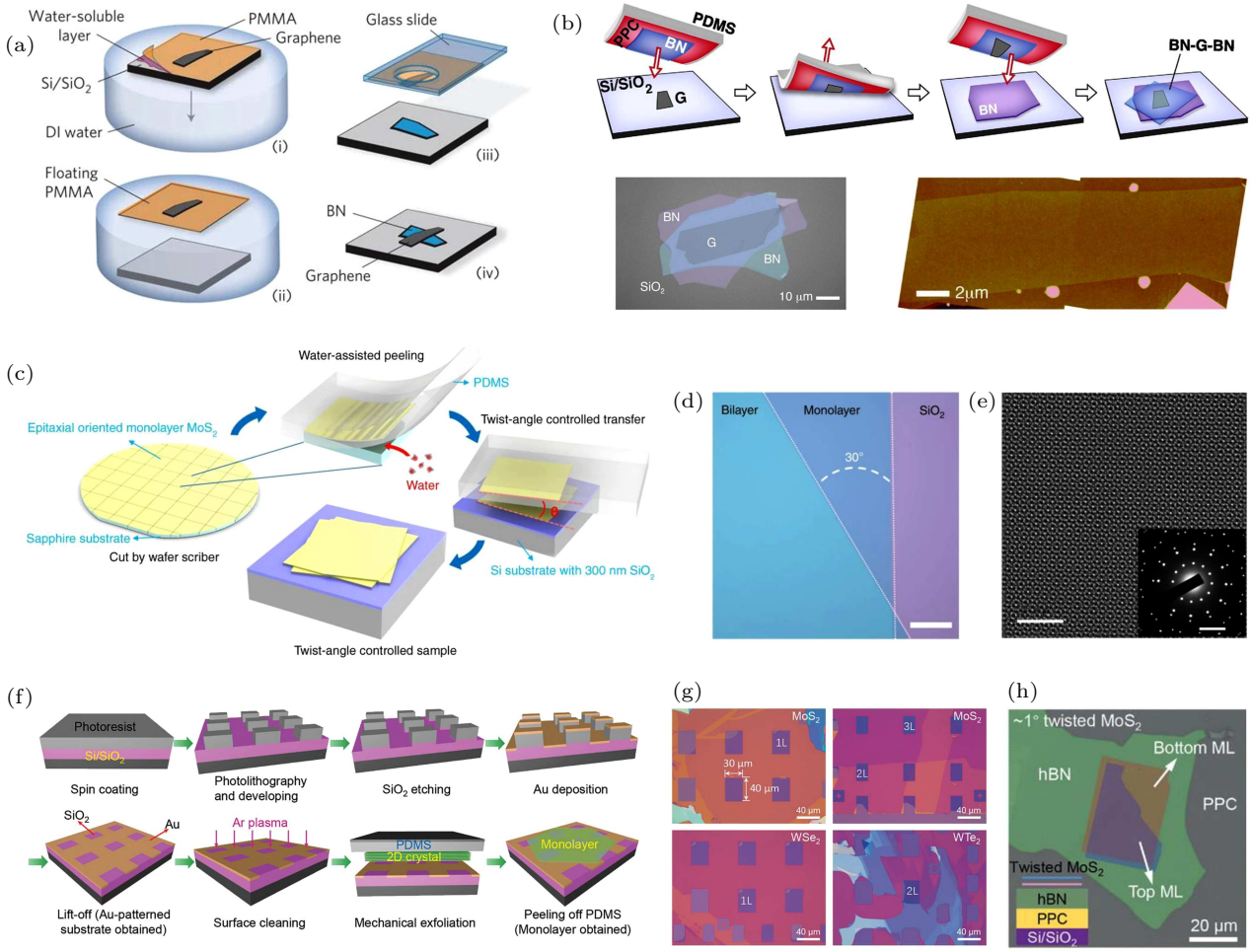


Fig. 3. Mechanical exfoliation and stack transfer technique. (a) Schematic illustration of the stack transfer process for fabricating graphene-on-hBN devices. Reproduced with permission from Ref. [50]. (b) Schematic of the vdW technique for polymer-free assembly of layered materials (top); optical image and atomic force microscope (AFM) image of a multilayered heterostructure (bottom). Reproduced with permission from Ref. [51]. (c) Schematic diagram of a corner multilayer MoS_2 moiré superlattice fabricated using the water-assisted method; optical micrograph, scale bar 300 μm (d) and STEM image (e) of a double-layer MoS_2 with 30° angle orientation, scale bar 3 nm; insert is electron diffraction pattern, scale bar 5 nm^{-1}. Reproduced with permission from Ref. [60]. (f) Schematic diagram of gold-assisted pick-up method for fabricating moiré superlattices. (g) Optical image of exfoliated large-area MoS_2, WSe_2 and WTe_2. (h) Optical image of approximately 1° twisted bilayer MoS_2 on hBN. Reproduced with permission from Ref. [61].

However, these methods result in moiré patterns with a high degree of randomness, making it difficult to precisely fabricate moiré superlattices. In 2018, building upon the pick-up method, Cao *et al.* introduced a rotation process, creating the tear–rotate–stack transfer method, which allows for precise control over the rotation angle, enabling the

fabrication of MATBG moiré superlattices.[24] Utilizing this method, researchers have successfully synthesized a range of homogeneous and heterogeneous moiré superlattices, including TTG,[47] TBBG,[52] twisted bilayer WSe_2 ($tWSe_2$),[53] twisted bilayer $MoTe_2$ ($tMoTe_2$)[54] as well as heterostructures like WS_2/WSe_2[55] and $MoSe_2/WSe_2$.[56] Nevertheless, since each unit cell of TMDCs contains three atomic layers, and the interaction with the substrate is primarily controlled by the surface atoms, the dipole interaction between the chalcogen atoms and the oxygen atoms in SiO_2 is relatively weak.[57] This makes it difficult for the conventional pick-up method to exfoliate large areas of TMDCs. Researchers have attempted to treat the SiO_2 surface with oxygen plasma to clean the substrate surface, but the exfoliation results are still not satisfactory.[58,59] Nonetheless, recently, Liao *et al.* employed the water-assisted peeling technique, and successfully achieved millimeter-scale multilayer MoS_2 heterojunctions.[60] The detailed transfer procedure is illustrated in Fig. 3(c). Figure 3(d) presents an optical micrograph of the transferred 30° rotated bilayer MoS_2, while Fig. 3(e) displays a scanning transmission electron microscope (STEM) image along with the corresponding electron diffraction pattern, clearly revealing a distinct moiré pattern. However, this method easily traps water molecules at the interface, and is prone to leaving residual adhesive, hence the need to develop new transfer techniques.

Researchers have been continuously refining this technology to achieve superior transfer outcomes. Wu *et al.* found that using a gold-assisted exfoliation method can enable the exfoliation of bulk TMDCs into 2D materials,[61] as shown in Fig. 3(f). This is due to the strong interaction between gold and the interlayer compounds, which can form quasi-covalent bonds similar to covalent bonding. Furthermore, this method can also be used to batch exfoliate TMDCs with different numbers of layers, as shown in Fig. 3(g). Afterward, by incorporating the tear-rotate-stack method, templated fabrication of moiré superlattices can be accomplished, as shown in Fig. 3(h). This method not only facilitates the exfoliation of 2D atomic layers with varying numbers of layers, but is also scalable, making it applicable to the fabrication of other 2D moiré superlattices.[62] However, gold atoms introduced on the surface are difficult to completely remove and can easily affect the intrinsic physical properties of 2D materials.

3.1.2. Large-scale size transfer techniques

While moiré superlattices fabricated by mechanical exfoliation transfer techniques exhibit high quality, their applications on an industrial scale are hindered by the limited sample sizes, which range from microns to millimeters. Therefore, researchers are actively pursuing methods to enable the large-scale transfer fabrication of moiré superlattices. In 2013, Martins *et al.* successfully demonstrated the direct transfer of large-area graphene onto flexible substrates through a heat-pressing method.[63] While this method is primarily suitable for flexible substrates and may not be as effective for other types of substrates. Furthermore, the Cu foil surface is often quite uneven, making it difficult to achieve close contact with the target substrate and potentially resulting in damage during the transfer process. Quellmalz *et al.* improved the contact between the target substrate and the as-grown sample by using bisbenzocyclobutene (BCB) as a surface adhesive. Subsequently, the sample was transferred onto the target substrate through a heat-pressing method. Repeating this process allowed for the fabrication of multilayer moiré superlattices, with the specific procedure shown in Fig. 4(a).[64] This scalable transfer technique is applicable to the fabrication of various multilayer moiré superlattices, including multilayer graphene moiré superlattices, graphene/hBN moiré superlattices, and multilayer TMDs moiré superlattices, as depicted in Figs. 4(b) and 4(c). However, the introduction of BCB in this transfer technique may affect the characterization of the physical properties of the moiré superlattices. Consequently, there remains a need for the development of new large-scale transfer technologies.

In 2022, Gao *et al.* utilized a multifunctional small molecule/PMMA/PDMS as a transfer medium to fabricate large-scale hBN/graphene/hBN moiré superlattices.[65] While the moiré superlattices fabricated by this method boast high quality and cleanliness, it is challenging for the small molecule layer to fully pick up the sample during the transfer process, which can lead to damage. Additionally, the adhesion strength between different samples and substrates varies, and the small molecule layer may not be universally applicable to other 2D materials. Simultaneously, Lu *et al.* used a thin layer of polyvinyl alcohol (PVA) as a transfer medium layer to fabricate moiré superlattices using high-κ dielectric 2D materials, as shown in Figs. 4(d) and 4(e). This fabrication method addresses the issues encountered by Gao *et al.* in the production of moiré superlattices. However, the process of removing PVA with plasma can damage the underlying sample, making it unsuitable for delicate 2D materials such as graphene and TMDs.[66]

In recent years, there have been breakthroughs in the technology for large-scale fabrication of moiré superlattices using wet transfer methods. Yuan *et al.* developed a proton-assisted flat-to-flat transfer method, achieving wafer-scale fabrication of twisted multilayer graphene moiré superlattices,[68] as shown in Figs. 4(f)– 4(j). This method utilizes rotation and heating to expel most of the trapped water at the graphene interfaces, followed by a hydrogen plasma process that fully cleans the surface and interface. The residuals on the graphene are more easily decomposed under hydrogen plasma, resulting in an extremely clean surface. This process also facilitates the decoupling of graphene from the substrate and the removal of residual water molecules between the graphene and the substrate. Moreover, by leveraging the wafer-flat alignment of graphene, they can control the twist angles and fabricate moiré superlattices of twisted multilayer graphene at vir-

tually any desired angle. Furthermore, this transfer method exhibits excellent scalability and can also be used to fabricate graphene/hBN moiré superlattices, TMDCs moiré superlattices, and so on.

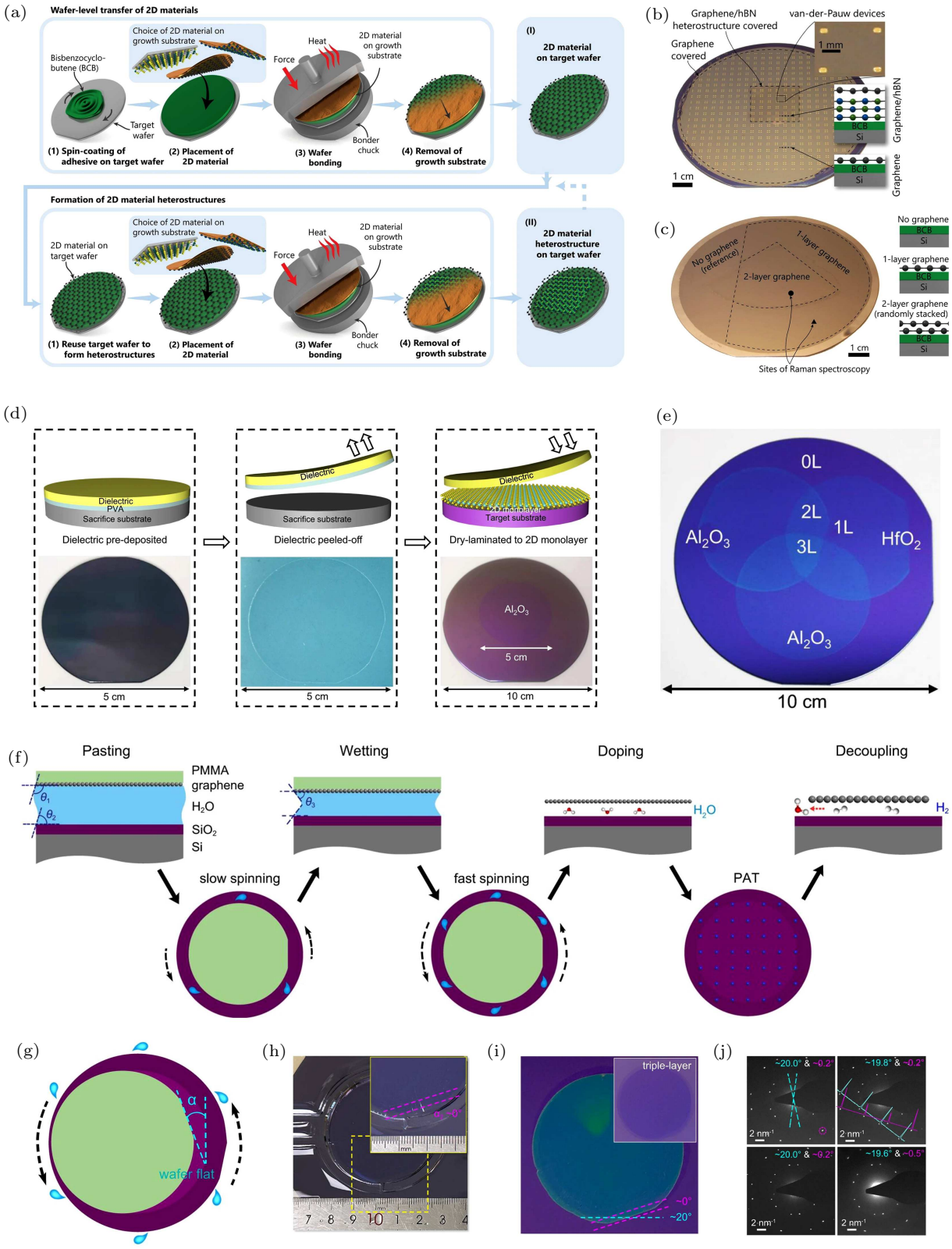


Fig. 4. Large-scale fabrication of moiré superlattices. (a) Schematic illustration of thermal pressing method for fabricating moiré superlattices. (b) Photograph of van der Pauw (vdP) devices. (c) Photograph of multilayer graphene superlattices. Reproduced with permission from Ref. [64]. (d) Schematics and optical images of wafer-scale dielectric lamination process with three steps. (e) Photograph of vdW $Al_2O_3/HfO_2/Al_2O_3$ oxide superlattices. Reproduced with permission from Ref. [67]. (f) The transfer process includes a two-step spinning-assisted dehydration process and a proton-assisted treatment (PAT) decoupling process. (g) Schematic of controlling the macroscopic stacking angle (α) of double-layer graphene by rotating the orientations of graphene wafer flats. (h) Adjusting the macroscopic stacking angle at $\sim 0^\circ$. (i) Graphene superlattices after spinning-assisted transfer process. (j) Selected area electron diffraction (SAED) patterns of the triple-layer graphene. Reproduced with permission from Ref. [68].

The proton-assisted flat-to-flat transfer technique for fabricating moiré superlattices is considered one of the most promising approaches for large-scale industrial production of moiré superlattices. However, the twist angles require more precise control. It is believed that the rotational transfer method will be able to achieve mass production of moiré superlattices once the angle control is improved.

Noting that the wafer-scale moiré superlattices usually use raw CVD grown samples as raw materials. Therefore, in the construction of the superlattices, the as-grown 2D materials must be stripped off from the growth substrate without damage. Currently, a variety of transfer methods have been developed, such as etching the growth substrate. For difficult-to-etch metal substrates, researchers have also developed methods such as the bubble method[69] and oxidizing substrates[70,71] to quickly separate samples, these previous large-scale transfer methods have laid the foundation for the fabrication process of moiré superlattices.

3.2. Growth preparation

Stack transfer technology, while being a complex process for moiré superlattice fabrication, frequently struggles to meet the standards for consistency and quality necessary for large-scale manufacturing. Therefore, researchers have begun to explore the direct growth method for fabricating moiré superlattices. An increasing number of methods for growing moiré superlattices are being reported, with the CVD method being the primary one. Additionally, other growth methods are also reported, including molecular beam epitaxy (MBE), solvothermal synthesis, and so on.

3.2.1. CVD method

The CVD method has been widely used for growth of various 2D materials and is currently one of the most promising approaches for large-scale growth of moiré superlattices. The moiré superlattices form through CVD direct growth, resulting in ultra-clean interfaces and high quality. In the following, we will provide a detailed introduction to the CVD methods for growing moiré superlattices from the aspects of controlling growth conditions, including gas adjustment, temperature control, substrate control, and compound-assisted regulation.

(I) Gas regulation of CVD grown moiré superlattices

The gas environment plays a crucial role in the CVD growth of moiré superlattices, as it is one of the key parameters for controlling the growth of moiré superlattices. Different gas environments can significantly affect the growth of 2D materials. In 2013, Wang *et al.* grew graphene/hBN vertical heterostructure on Cu foils by altering the composition of the gaseous precursors and sequentially introducing volatile ammonia borane gas and methane.[72] At the same time, Shi *et al.* successfully grew MoS_2 on a graphene/Cu substrate by introducing a carrier gas into a mixed solution of ammonium thiomolybdate, forming a MoS_2/graphene vertical heterostructure.[73] This method of directly changing the composition of gaseous precursors to prepare moiré heterostructures makes it difficult to grow a uniform moiré pattern, hence there is a need for a novel method to regulate the growth.

Peng's research group successfully prepared homo-site twisted bilayer and trilayer graphene with angles of 0° and 30° by almost using a pure H_2 environment and increasing the gas flow rate under low pressure,[74] as shown in Fig. 5(a). They consider that growth kinetic conditions are one of the key factors in determining the formation of twisted angles. The change in gas flow rate disrupts the inherent growth kinetic conditions, allowing for the overcoming of higher energy barriers, thus making the appearance of twisted angles more likely. Liu *et al.* grew a series of homo-site twisted bilayer graphene with twist angles ranging from 0° to 30° on the surface of liquid Cu by placing a solid quartz rod inside a quartz tube,[75] which altered the gas flow rate and gas concentration distribution, as shown in Fig. 5(b). In addition to the growth of twisted graphene moiré superlattices, researchers have also grown TMDCs moiré superlattices by altering kinetic conditions. Xu *et al.* grew a series of homo-site twisted bilayer WS_2 with twist angles ranging from 0° to 120° on a SiO_2/Si substrate by tilting the substrate, which induced airflow disturbances and created a gradient distribution of precursor concentrations,[76] as shown in Fig. 5(c). Meanwhile, Li *et al.* established perturbed growth conditions by adjusting the spatial distribution of airflow near the substrate and the concentration of local reactants, resulting in the growth of high-quality homosite and hetero-site bilayer MoS_2.[77] These experimental phenomena further confirm that changing the state of airflow can disrupt the balance of growth kinetics, thereby making the control of the growth of twisted moiré superlattices possible.

In order to explore the impact of airflow environments on the growth of moiré superlattices, countless researchers have conducted numerous meticulous experiments in search of regulatory patterns. Sun *et al.* discovered through experiments that without the introduction of airflow disturbances, bilayer graphene has identical nucleation points and selectively grows AB-stacked bilayer graphene.[34] However, when CH_4 and H_2 are suddenly increased to cause airflow disturbances, hetero-site bilayer graphene is more likely to form, as shown in Fig. 5(d). A series of hetero-site bilayer graphene moiré superlattices with twist angles ranging from 0° to 30° have been grown using this method, as shown in Fig. 5(e). The influence of airflow on the growth of TMDCs moiré superlattices system has also been explored. Recently, Zhou *et al.* found that during the growth stage of MoS_2, introducing regular airflow disturbances could lead to the growth of homo-site bi-

layer MoS_2; whereas irregular airflow disturbances tended to result in the growth of hetero-site bilayer MoS_2, as shown in Figs. 5(f) and 5(g).[78] It is thought that the disturbance of airflow alters the growth microenvironment, disrupting the equilibrium state, thus making the formation of twisted moiré superlattices more likely. However, irregular gas disturbances cause changes in the nucleation points, leading to the formation of hetero-site moiré superlattices.

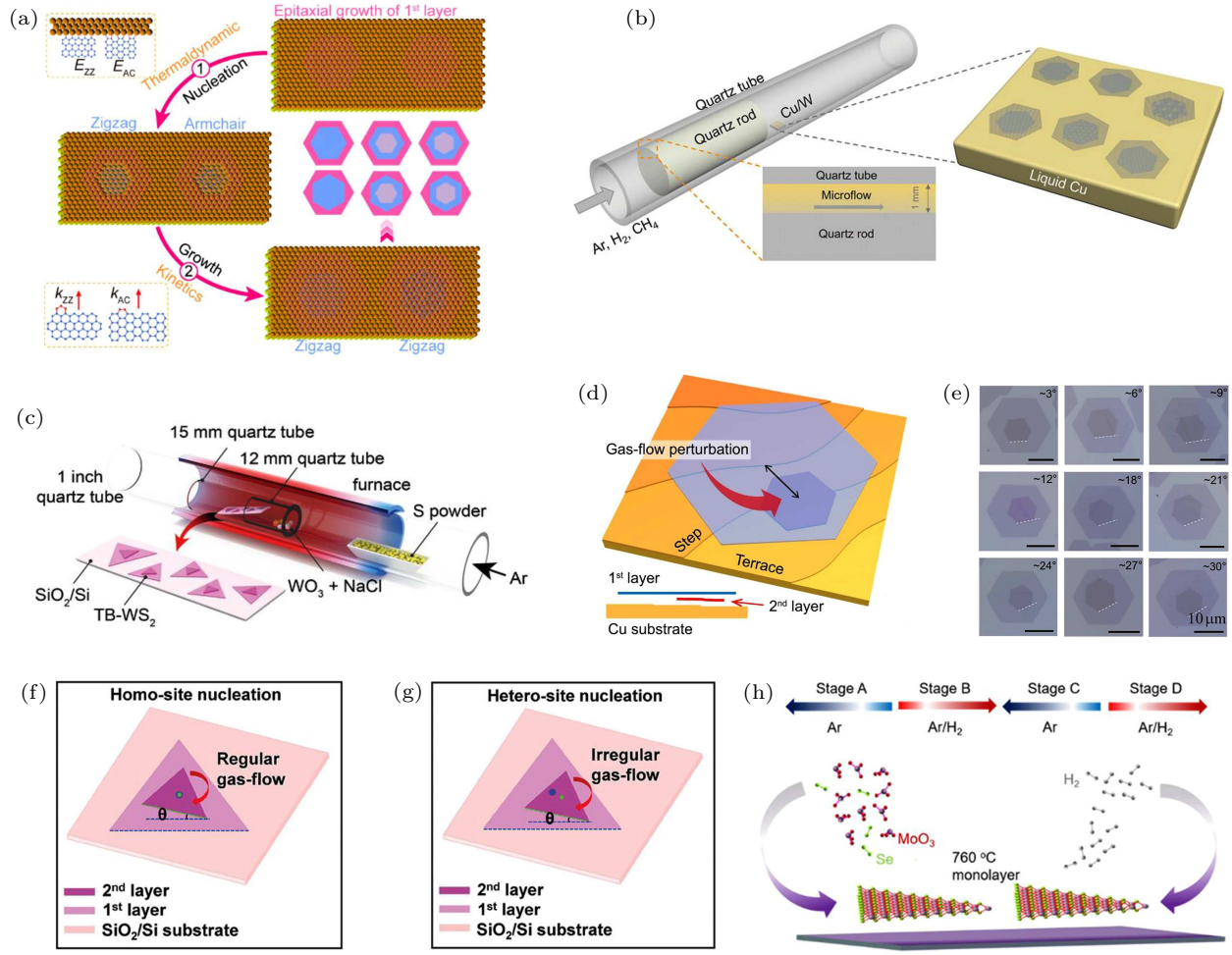


Fig. 5. Gas adjustment for the growth of moiré superlattices. (a) Schematic illustration of the growth of homo-site graphene moiré superlattices. Reproduced with permission from Ref. [74]. (b) Schematic of the designed CVD reactor for the growth of TBG. Reproduced with permission from Ref. [75]. (c) The growth of homo-site bilayer WS_2 moiré superlattices. Reproduced with permission from Ref. [76]. (d) Schematic of the growth of hetero-site graphene moiré superlattices. (e) Photograph of as-grown TBG. Reproduced with permission from Ref. [34]. The growth of homo-site (f) and hetero-site (g) MoS_2 moiré superlattices. Reproduced with permission from Ref. [78]. (h) Regulation of $MoSe_2$ moiré superlattice growth through airflow direction control. Reproduced with permission from Ref. [79].

In addition to the impact of airflow magnitude disturbances on the growth of moiré superlattices, frequent changes in the direction of airflow can also affect the growth of moiré superlattices. Peng *et al.* discovered that during the heating process, employing reverse airflow could prevent unintended nucleation, and then reintroducing forward airflow during the growth process enabled the precursors to uniformly nucleate on the substrate surface, which is beneficial for growing directionally consistent $MoSe_2$ moiré superlattices,[80] as shown in Fig. 5(h). Simultaneously, Zhang *et al.* prepared high-quality twisted bilayer MoS_2 (t-MoS_2) moiré superlattices using a similar method.[79] In summary, airflow control is one of the key parameters for the growth of moiré superlattices. By regulating the magnitude and direction of airflow to create disturbances, it is possible to control the growth of moiré superlattices.

(II) Temperature regulation of CVD grow moiré superlattices

Temperature is one of the most critical parameters in the CVD growth of 2D materials. In addition to a high flux being able to overcome the barrier for vertical growth of 2D materials,[81] temperature also provides the energy necessary for the growth of moiré superlattices. Gong *et al.* successfully grew lateral and vertical WS_2/MoS_2 heterojunctions in 2014 through a one-step growth strategy, as shown in Fig. 6(b).[82] They found that at a temperature of approximately 650 °C, the growth of lateral WS_2/MoS_2 heterojunctions is dominant; when the temperature is around 850 °C, it is easier to grow ver-

tical WS_2/MoS_2 heterojunctions, as shown in Fig. 6(a). Gong *et al.* considered that at low temperatures, kinetic effects are dominant, making it very difficult for WS_2 to nucleate and grow on the surface of MoS_2, while the energy required for WS_2 to bond and grow at the edges of MoS_2 is lower. At high temperatures, thermodynamic effects are dominant, and WS_2 has enough energy to overcome the barrier to nucleate and grow on the surface of MoS_2, thus facilitating the formation of vertical heterojunctions.

Besides the TMDCs system exhibiting this pattern, the growth of moiré superlattices in the graphene system is also affected by temperature. One year later, Gao *et al.* grew graphene on an hBN/Cu substrate, forming a graphene/hBN moiré superlattice.[83] They found that when the temperature exceeds 900 °C, lateral graphene/hBN heterojunctions are more likely to form; conversely, when the temperature is below 900 °C, vertical graphene/hBN heterojunctions are more readily formed. Thus, the growth of vertical heterojunctions in different 2D material systems varies in its dependence on temperature, often requiring the temperature to be determined based on the intrinsic properties of the materials themselves.

The one-step growth method for moiré heterostructures often requires very high temperatures to overcome the barriers to nucleation and growth, and it is difficult to avoid the formation of alloy compounds and lateral heterojunctions. Therefore, researchers have invented a two-step growth method for moiré superlattices. Yang *et al.* firstly grew high-quality single-crystal WSe_2 on the substrate at 1100 °C using WSe_2 powder; then at 600 °C, they epitaxially grew SnS_2 on WSe_2 using sulfur powder and SnO_2 powder, forming a SnS_2/WSe_2 moiré superlattice, as shown in Fig. 6(c).[84] Figure 6(d) shows the moiré superlattice of SnS_2/WSe_2, and Fig. 6(e) displays the moiré pattern formed in the SnS_2/WSe_2 moiré superlattice, where the lattice period of the moiré superlattice is 2.24 nm. Additionally, besides the three-atomic-layer TMDCs system moiré superlattices, five-atomic-layer TMDCs moiré superlattices can also be grown using a two-step method. Liu *et al.* firstly grew monolayer WSe_2 and MoS_2 in a high-temperature environment and then used them as substrates to grow Bi_2Te_3 and Sb_2Te_3 in a low-temperature environment respectively, forming Bi_2Te_3/WSe_2 and Sb_2Te_3/MoS_2 moiré superlattices.[85,86] Moreover, Zhang *et al.* directly used WSe_2 and In_2Se_3 powders through a two-step growth method: firstly grew a monolayer of WSe_2 at 1000 °C, and then epitaxially grew In_2Se_3 on WSe_2 at 700 °C, forming an In_2Se_3/WSe_2 moiré superlattice.[87] In addition, researchers have also attempted to firstly grow the bottom 2D material at low temperatures and then grow the top 2D material at high temperatures, trying to form moiré superlattices. Gong *et al.* firstly grew $MoSe_2$ in a low-temperature environment, and then grew WSe_2 in a high-temperature environment, finding that lateral and vertical heterojunctions coexisted.[88] This is due to the fact that in a high-temperature environment, the atomic energy of $MoSe_2$ grown in a low-temperature environment increases, becoming more active, and is more likely to bond with WSe_2 at the edges, forming lateral heterojunctions.

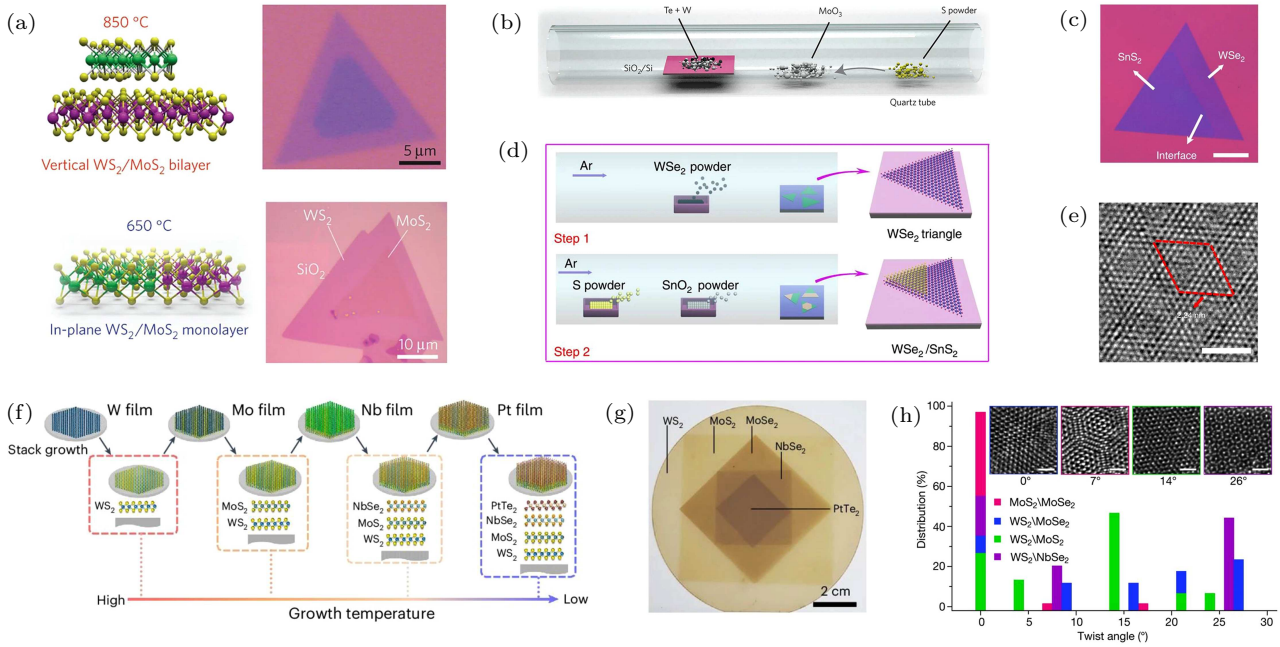


Fig. 6. Temperature control for growing moiré superlattices. (a) Schematic and optical images of WS_2/MoS_2 vertical heterojunctions and lateral heterojunctions. (b) Schematic of one-step growth of WS_2/MoS_2 heterostructures. Reproduced with permission from Ref. [82]. (c) Optical images of SnS_2/WSe_2 heterojunction, scale bar 200 μm. Schematic of two-step growth method (d) and moiré pattern (e) of SnS_2/WSe_2 moiré superlattices, scale bar 2 nm. Reproduced with permission from Ref. [84]. (f) Schematic of a temperature gradient strategy for the growth of TMDCs heterojunctions. (g) Wafer-scale $WS_2/MoS_2/MoSe_2/NbSe_2/PtTe_2$ heterojunctions. (h) The proportion of moiré superlattices with different twist angles. Reproduced with permission from Ref. [89].

The growth of high-quality moiré superlattices often begins with the growth of the underlying 2D materials that require high growth temperatures, followed by the growth of the top 2D materials that require lower growth temperatures. Based on this, Zhou *et al.* developed a strategy for growing multilayer vertical heterojunctions using a temperature gradient, as shown in Fig. 6(f).[89] They constructed more than 25 types of wafer-scale moiré superlattices, with the layer number of moiré superlattices reaching up to five, such as $WS_2/MoS_2/MoSe_2/NbSe_2/PtTe_2$, as shown in Fig. 6(g). Additionally, Zhou *et al.* also obtained the twist angle statistical distribution of the moiré superlattices, as shown in Fig. 6(h). In summary, temperature is one of the key factors in the growth of moiré superlattices, and a high-to-low temperature strategy can be employed to achieve large-scale growth of moiré superlattices. However, since the high-to-low temperature approach dictates the stacking growth sequence of the moiré superlattice, this growth strategy also exhibits certain limitations.

(III) Substrate selection of CVD grown moiré superlattices

Growth substrate is another critical factor to affect the growth of 2D materials. The type of substrate material, catalytic activity, surface morphology, geometric structure and even the lattice orientation can significantly impact the growth of moiré superlattices.[90] For example, Zhang *et al.* successfully grew a graphene/hBN vertical heterostructure on a Ni film by using the catalytic ability of the substrate and the precipitation mechanism of growth,[91] as shown in Fig. 7(a). Firstly, they sequentially deposited a Ni film, (B, N) source, and a C-doped Ni film on a SiO_2/Si substrate, followed by annealing in a high vacuum environment. Carbon atoms near the surface precipitated on the surface first, and then B and N atoms diffused to the substrate surface to nucleate and grow, ultimately forming a graphene/hBN moiré superlattice, as shown in Fig. 7(b). This method, due to the unevenness of the deposited substrate, makes it difficult to grow high-quality moiré superlattices. A year later, Fu *et al.* grew high-quality MoS_2/hBN moiré superlattices on a Ni-Ga alloy/Mo foil substrate, as shown in Fig. 7(d).[92] They firstly placed the Ni-Ga alloy on top of the Mo foil and then performed high-temperature annealing to ensure close contact between the Ni-Ga alloy and the Mo foil. Subsequently, they introduced ammonia borane precursors to grow an hBN thin film on the Ni-Ga alloy substrate, and then switched the precursors of H_2S to grow MoS_2 on top of the hBN film, forming a MoS_2/hBN moiré superlattice, as shown in Fig. 7(c). Due to the diffusion of Mo atoms to the substrate surface at high temperatures, followed by their permeation through the hBN and reaction with S atoms on the hBN surface to form MoS_2, this method has addressed the issue of substrate surface roughness. However, the non-uniform diffusion of Mo atoms across the hBN surface makes it difficult to create large-area uniform moiré superlattices, necessitating the development of new growth techniques.

Researchers have attempted to change the surface morphology and geometric shape of the substrate to enable epitaxial growth of 2D materials on the surface to form moiré superlattices. Bierman *et al.* firstly discovered the growth of PbS helical tree-like nanowires in materials with screw dislocations,[93] sparking a surge in the growth of nanomaterials on substrates with screw dislocations. In 2018, Tay *et al.* studied the impact of flat substrates and substrates with screw dislocations on the growth of graphene.[94] They found that the growth of graphene on a typical flat substrate follows an interfacial nucleation mechanism and the growth of few-layer graphene proceeds from top to bottom. However, on a substrate with screw dislocations, the growth of graphene is driven by the screw dislocations, with graphene epitaxially growing from bottom to top along the trajectory of the screw dislocations, thus making it easier to form twisted graphene moiré superlattices. In 2020, Zhao *et al.* grew twisted multilayer WS_2 moiré superlattices and twisted multilayer WSe_2 moiré superlattices on substrates with screw dislocations, and they found that the twist angles of the grown moiré superlattices varied with different screw dislocation angles,[95] as shown in Figs. 7(e)–7(h). Microscopic structural analysis reveals a direct correspondence between the crystal lattice twist and the geometric torsion of the layers, resulting in the formation of moiré superlattices at the interlayer interfaces. In addition, researchers have also grown moiré superlattices of MoS_2,[96] SnSe,[97] Sb_2Te_3,[98] SnS,[99] and others on substrates with screw dislocations.

The orientation of the substrate can also affect the growth of moiré superlattices. Recently, Liu's research group has been able to grow twisted bilayer graphene with designed angle through ingenious structural design.[100] Firstly, they cut the Cu(111) copper foil into two parallel-edged segments, then aligned one vertex and rotated it by any angle. Subsequently, they used the CVD method to epitaxially grow graphene between the two copper foils, then increased the temperature to obtain bilayer graphene with the designed twist angle, and finally etched the copper foil to separate the bilayer graphene with the designed twist angle, as shown in Fig. 7(i). Figures 7(j) and 7(k) present the TEM images and electron diffraction patterns of the 30° twisted bilayer graphene, respectively. However, this growth method is currently limited to materials of graphene, and new growth methods need to be developed for other types of moiré superlattices. In summary, the substrate plays an essential role in the growth regulation of moiré superlattices, and altering the substrate approach can introduce new variables to control the growth of moiré superlattices.

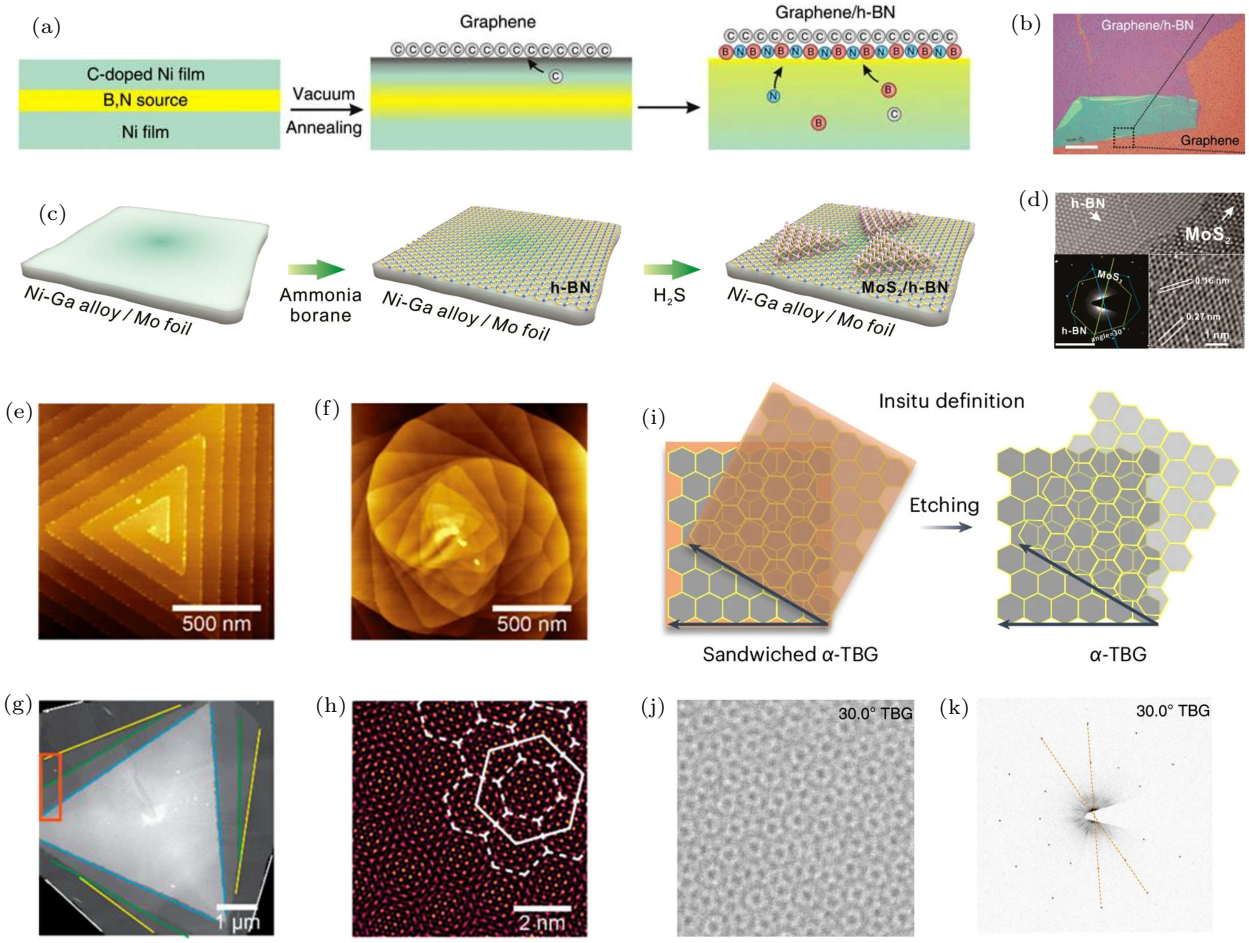


Fig. 7. Substrate control for the growth of moiré superlattices. (a) Schematic illustration of the co-segregation growth process for graphene/h-BN heterostructures. (b) Optical images of the as-grown sample transferred to a SiO_2/Si substrate. Reproduced with permission from Ref. [91]. (c) Surface catalysis and precipitation mechanism on the substrate for the growth of MoS_2/hBN moiré superlattices. (d) TEM images of MoS_2/h-BN heterostructures. Reproduced with permission from Ref. [92]. AFM images of aligned WS_2 spirals grown on flat substrates (e) and screw dislocation substrates (f). (g) STEM image of a super-twisted WS_2. (h) moiré patterns of WS_2 superlattices. Reproduced with permission from Ref. [95]. (i) Schematic for the growth TBG with designed angle. moiré patterns (j) and SAED patterns (k) of 30° TBG. Reproduced with permission from Ref. [100].

(IV) Compound-assisted regulation of CVD grown moiré superlattices

Compound-assisted growth plays a significant role in the growth of 2D materials, as it can reduce the melting temperature of precursors and even lower the formation energy of vertical heterostructures, thereby accelerating the growth of 2D materials.[101] In 2015, Li *et al.* firstly used alkali metal halides to assist in the regulation of the growth of 2D TMDCs, resulting in the growth of high-quality, large-scale monolayer WS_2 and WSe_2.[102] This is due to the chemical reaction between the tungsten oxide precursor and the alkali metal compounds, forming low-melting-point tungsten oxyhalides, which can promote the nucleation and growth of WS_2 and WSe_2 in a high-temperature environment.[103] Since then, a wave of research on salt-assisted control of the growth of 2D materials has been initiated. Using the salt-assisted growth strategy, researchers have also grown high-quality, large-area monolayers of MoS_2,[104] $MoSe_2$,[105] SnS_2,[106] $NbSe_2$,[107] and so on.

Furthermore, the compound-assisted method is also used to regulate the growth of moiré superlattices. In 2018, Fu *et al.* mixed the precursor with NaCl and, using a one-step growth method, successfully prepared NbS_2/MoS_2 moiré superlattices.[108] Moreover, Xia's research group grew large-area, high-quality $WS_ySe_{2-y}/WS_xSe_{2-x}$ moiré superlattices using a salt-assisted and two-step growth method, as shown in Figs. 8(a) and 8(b).[109] The primary purpose of using NaCl-assisted growth is to lower the melting and boiling points of the precursor materials, making it easier for the precursors to vaporize and then deposit onto the substrate for nucleation and growth.

In addition to using alkali metal halides, researchers have also discovered other types of compound-assisted methods for growing moiré superlattices. Shao *et al.* successfully grew twisted bilayer WS_2 moiré superlattices with a twist angle of 60° by introducing tin (Sn) atoms, as shown in Fig. 8(c).[110] The interlayer introduction of Sn significantly facilitates the formation of a 60° twisted bilayer structure by diminishing the interlayer stacking energy barrier. In the absence of Sn, the 0° arrangement of layers turned out to be the most stable, requiring less energy than the 2H phase. However, when Sn was present, the 60° layer arrangement with the 2H phase became

the most stable. Additionally, researchers have improved this method and obtained new approaches for growing moiré superlattices. Zheng *et al.* utilized SnO_2 and KOH to assist in the growth of twisted bilayer WSe_2 moiré superlattices, as shown in Fig. 8(d).[111] They successfully grew twisted bilayer WSe_2 moiré superlattices with a small angle of 1.5°, as depicted in Fig. 8(e). Researchers think that KOH can promote the preferential growth of 2D materials, facilitating the growth of the second layer.

In addition to the type of salt affecting the growth of moiré superlattices, the amount of salt also influences the growth of moiré superlattices. Recently, Xu *et al.* systematically investigated the impact of the ratio of NaCl salt to precursors on the growth of MoS_2 moiré superlattices,[112] as shown in Figs. 8(f) and 8(g). They found that a high salt ratio could promote the rapid growth of moiré superlattices, which is due to the increase in the size and density of nucleation in a high salt ratio environment, making it easier to form bilayer or multilayer MoS_2. Therefore, by controlling the salt ratio, one can regulate the nucleation density and size of nuclei to grow large-area, high-quality moiré superlattices. In summary, compound-assisted growth is an important means of regulating the growth of moiré superlattices. By synergistically controlling different influencing factors and introducing new variables that can be fine-tuned to control the structural properties and alignment of the superlattices, thereby enhancing the quality and uniformity. It is believed that more universal methods for growing moiré superlattices will emerge in the future.

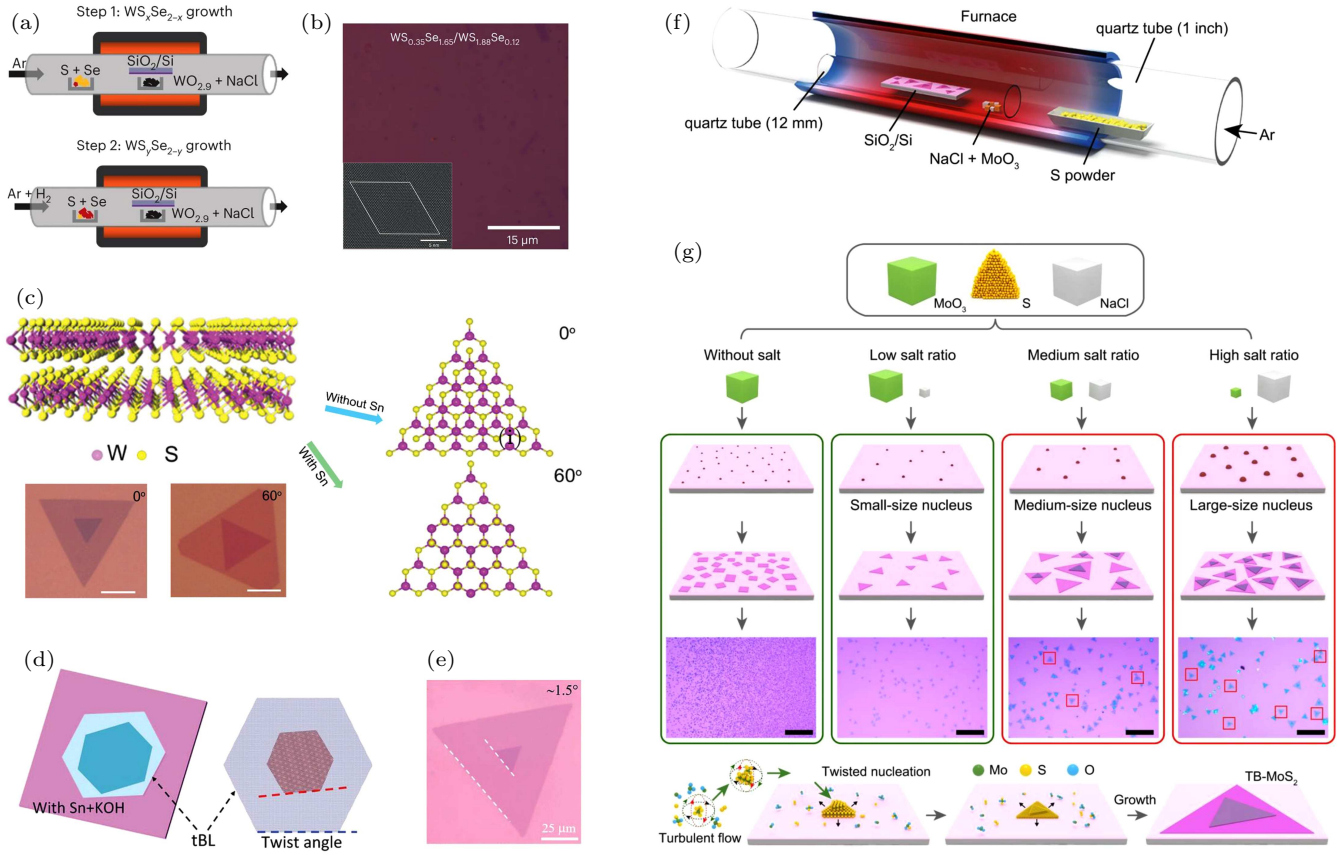


Fig. 8. Compound-assisted regulation for growing of moiré superlattices. (a) Schematic illustration of salt-assisted growth of $WS_ySe_{2-y}/WS_xSe_{2-x}$ moiré superlattices. (b) Photograph and STEM image of $WS_ySe_{2-y}/WS_xSe_{2-x}$ moiré superlattices. Reproduced with permission from Ref. [109]. (c) Schematic illustration of SnO_2-assisted growth method and optical images of bilayer WS_2 moiré superlattices. Reproduced with permission from Ref. [110]. (d) Growth of bilayer WSe_2 moiré superlattices assisted by SnO_2 and KOH. (e) Optical image of approximately 1.5° $tWSe_2$. Reproduced with permission from Ref. [111]. (f) Illustration of the CVD setup for the synthesis of twisted bilayer MoS_2. (g) Growth of MoS_2 moiré superlattices with varying NaCl ratios. Reproduced with permission from Ref. [112].

3.2.2. Other direct growth and synthesis method

Molecular beam epitaxy (MBE) is an epitaxial technique used for growing superlattice structures, allowing for precise control over composition and doping distribution on a nanoscale. MBE grows superlattices within an ultra-high vacuum (UHV) chamber, thereby ensuring a pristine environment essential for the epitaxial process.[113] The UHV conditions enable precise control of the growth rate, making MBE particularly well-suited for growing complex structures with both small ($< 2\%$–3%) and large lattice mismatch. This capability facilitates the fabrication of 2D structures with incredibly smooth, atomic-level surfaces.[114] Therefore, MBE is also a crucial technique for the growth of moiré superlattices. For instance, in 2020, Kezilebieke *et al.* grew a $CrBr_3/NbSe_2$ moiré superlattice using the MBE method and observed the phenomenon of topological superconductivity.[115] The fol-

lowing year, Zhao *et al.* grew a 1T-$TiTe_2$/1T-$TiSe_2$ moiré superlattice using this method,[116] and they discovered the enhanced charge density wave state phenomenon. In addition to growing TMDCs moiré superlattices, MBE can also be used to grow graphene-based moiré superlattices. Pham *et al.* used the MBE method to grow $MoTe_2$/graphene moiré superlattices on the SiC substrate.[117] Moiré superlattices grown using the MBE method have extremely clean atomic layer interfaces and very high quality.

However, compared to CVD samples, they are very unstable in atmospheric environments. Moreover, achieving precise angle control remains a challenge in the current MBE growth process for moiré superlattices. Additionally, a key feature of MBE technology is its extremely low growth rate,[118] typically only a few angstroms per second, which results in a relatively low yield for MBE, making it challenging to achieve large-scale commercial production.

Apart from the epitaxial techniques of CVD and MBE for direct growth 2D moiré superlattices, solvothermal synthesis is another direct synthesis method. This method involves the fabrication of materials through chemical reactions within a closed environment, employing organic solvents or non-aqueous solvents as the reaction medium at specific temperatures and pressures.[119] For example, Gong *et al.* synthesized MoS_2/graphene moiré superlattices using graphene oxide and $(NH_4)_2MoS_4$ through a solvothermal synthesis.[120] At the same time, Yu *et al.* synthesized MoS_2/graphene moiré superlattices using a similar method,[121] which exhibited highly efficient and stable electrocatalytic properties. The stable reaction conditions of the solvothermal synthesis method allow for the batch production of moiré superlattices. However, due to the small size of the synthesized moiré superlattices, they are difficult to apply in practical applications.

3.3. Tip manipulation method for accurate twist angle

The properties of moiré superlattices manifest within a narrow twist angle range of $\pm 0.1^\circ$,[122] making precise control of the twist angle crucial. However, directly grown moiré superlattices exhibit a wide range of interlayer twist angles, posing a significant challenge for precise control. Additionally, stacked transfer techniques still struggle to achieve accurate control within this small range. Here, we will further introduce the tip manipulation method for preparing moiré superlattices, which enables precise control within such a narrow range.

Tip manipulation, a prevalent method in dynamic manipulation, entails the precise folding or rotation of 2D atomic layer materials using a tip to fabricate moiré superlattices.[123] For example, Liao *et al.* obtained MoS_2/graphene moiré superlattices by rotating triangular MoS_2 on graphene by arbitrary angles with an accuracy of 0.1° using AFM tip manipulation,[124] as shown in Figs. 9(a) and 9(b). Furthermore, Dean's team used the identical technique to accurately rotate hBN atop graphene at arbitrary angles with an accuracy of 0.2°, producing hBN/graphene moiré superlattices at rotation angles of 0°, 45°, and 70°.[125] Likewise, Hu *et al.* leveraged AFM for the precise manipulation of *in situ* rotation in twisted bilayer graphene.[126]

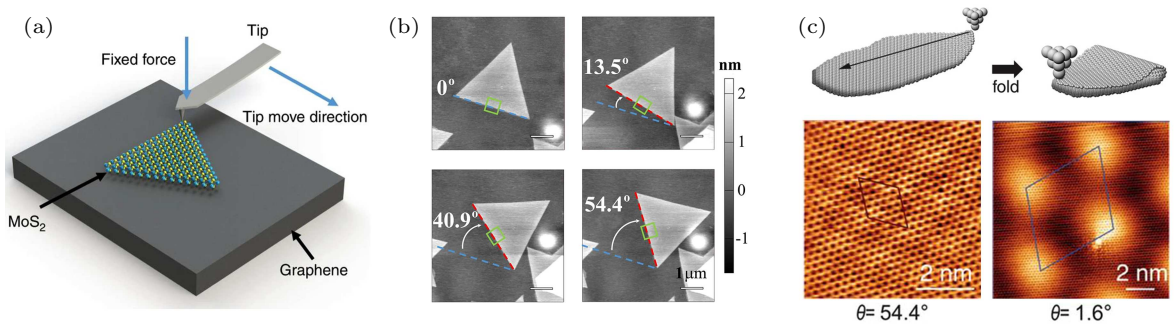


Fig. 9. Tip manipulation for fabricating moiré superlattices. (a) Schematic illustration of MoS_2 rotation on graphene via AFM-tip manipulation. (b) AFM images of the MoS_2/graphene Moiré superlattices. Reproduced with permission from Ref. [124]. (c) Schematic of Moiré superlattices fabricated with an STM tip (top) and STM images of graphene moiré superlattices (bottom). Reproduced with permission from Ref. [127].

In addition to rotational manipulation via AFM tips, STM tip manipulation also serves as a dynamically adjustable technique for preparing moiré superlattices. Gao's research team employed STM tips to fold graphene nanoislands in arbitrary directions, creating TBG with adjustable rotation angles ranging from 0° to 60° and an angular precision of 0.1°.[127] Figure 9(c) displays STM images of the TBG prepared with rotations of 54.4° and 1.6°, where the moiré patterns are distinctly visible. However, tip manipulation is highly dependent on sophisticated equipment and advanced techniques, thus incurring significant costs. Moreover, the moiré superlattices constructed by this method are typically small in size, making them unsuitable for large-scale fabrication and application.

4. Summary and outlook

The advent of 2D materials and vdW heterostructures has granted us an unparalleled capacity to innovate and engineer novel materials. The researchers used lattice dislocation or rotational distortion in 2D materials to design moiré super-

lattices, enabling precise control of their band structure and revealing a large number of interesting physical phenomena. The precise and controllable preparation of high-quality superlattices is the foundation of future physical property development and application exploration. This review systematically introduces the fabrication methods of moiré superlattices, including the stacked transfer techniques, direct growth methods and tip manipulation. It mainly explores in detail the impact of the gas environment, temperature, substrate, and compound-assisted regulation on the CVD growth of moiré superlattices.

In general, although numerous transfer methods for preparing moiré superlattices have been developed, significant challenges remain in scaling up production while maintaining high-quality production. Issues such as structural degradation, interface contamination, and the uneven and inaccurate angle control continue to impact the physical properties of moiré superlattices. While the pick-up transfer technique excels in preserving clean interfaces, it is prone to generating bubbles, inconsistent angular misalignment, and struggles with large-area fabrication. The proton-assisted method provides an effective means to obtain wafer-scale moiré superlattices with clean interface, but it lacks precise twistangle control. Further research should focus on obtaining high-quality ultra-uniform raw materials, developing large-size and high-precision transfer platforms, and integrating the advantages of various existing transfer methods.

CVD is currently the most promising method for large-scale growth moiré of superlattices, and the obtained moiré superlattices have an ultra-clean surface and very high quality. However, challenges remain in achieving uniform multilayer superlattice and precisely controlling interlayer twist angles. Additionally, the growth temperature constraints of 2D materials limit the range of moiré superlattices that can be grown. Relying solely on individual gas control, temperature regulation, substrate tuning, and compound assistance is insufficient to overcome the aforementioned challenges, researchers need to comprehensively adjust to achieve high-quality, large-area CVD growth of moiré superlattices by comprehensively regulating these variables and introducing new controls in the future.

Acknowledgements

Project supported by the National Natural Science Foundation of China (Grant Nos. 52425203 and 12104218), the the Natural Science Foundation of Jiangsu Province (Grant Nos. BK20240008 and BK20241252), the China National Postdoctoral Program for Innovative Talents (Grant No. BX2021120), the Xiaomi Foundation, the Postdoctoral Fellowship Program of CPSF (Grant No. GZC20231093), and Jiangsu Funding Program for Excellent Postdoctoral Talent (Grant No. 2023ZB553).

References

[1] Novoselov K S, Geim A K, Morozov S V, Jiang D, Zhang Y, Dubonos S V, Grigorieva I V and Firsov A A 2004 *Science* **306** 666
[2] Lin H H, Zhu Q, Shu D H, Lin D J, Xu J, Huang X L, Shi W, Xi X X, Wang J W and Gao L B 2019 *Nat. Mater.* **18** 602
[3] Liu L, Li T T and Ma L 2022 *Nature* **605** 69
[4] Qin B, Ma C J and Guo Q L 2024 *Science* **385** 99
[5] Xia Y, Chen X Y, Wei J C, Wang S Y, Chen S Y, Wu S M, Ji M B, Sun Z Z, Xu Z H, Bao W Z and Zhou P 2023 *Nat. Mater.* **22** 1324
[6] Xue G D, Zhou Z Q and Guo Q L 2024 *Science* **384** 1100
[7] Chen T A, Chuu C P, Tseng C C, Wen C K, Wong H S P, Pan S Y, Li R T, Chao T A, Chueh W C, Zhang Y F, Fu Q, Yakobson B I, Chang W H and Li L J 2020 *Nature* **579** 219
[8] Fukamachi S, Solis-Fernández P, Kawahara K, Tanaka D, Otake T, Lin Y C, Suenaga K and Ago H 2023 *Nat. Electron.* **6** 126
[9] Ma K Y, Zhang L, Jin S, Wang Y, Yoon S I, Hwang H, Oh J, Jeong D, Wang M, Chatterjee S, Kim G, Jang A R, Yang J, Ryu S, Jeong H Y, Ruoff R S, Chhowalla M, Ding F and Shin H S 2022 *Nature* **606** 88
[10] Wang L, Qi J J and Wei W Y 2024 *Nature* **629** 74
[11] Wang Y N, Zhao C, Gao X, Zheng L M, Qian J, Gao X Y, Li J D, Tang J C, Tan C W, Wang J H, Zhu X T, Guo J D, Liu Z F, Ding F and Peng H L 2024 *Nat. Mater.* **23** 994
[12] Chen C, Yin Y L and Zhang R C 2023 *Nat. Mater.* **22** 717
[13] Cording L, Liu J W, Tan J Y, Watanabe K, Taniguchi T, Avsar A and Özyilmaz B 2024 *Nat. Mater.* **23** 479
[14] Kim S, Myeong G, Shin W, Lim H, Kim B, Jin T, Chang S, Watanabe K, Taniguchi T and Cho S 2020 *Nat. Nanotechnol.* **15** 203
[15] Li W Y, Tao Q Y, Li Z W, Yang G H, Lu Z Y, Chen Y, Wen Y, Wang Y L, Liao L, Liu Y and He J 2024 *Nat. Electron.* **7** 131
[16] Wu Z H, Lyu Y X, Zhang Y, Ding R, Zheng B N, Yang Z B, Lau S P, Chen X H and Hao J H 2021 *Nat. Mater.* **20** 1203
[17] Cao F C, Zhang Y, Wang H Q, Khan K, Tareen A K, Qian W J, Zhang H and Ågren H 2022 *Adv. Mater.* **34** 2107554
[18] Li D Q, Zheng W H and Gali S M 2024 *Nat. Mater.* **23** 1085
[19] VahidMohammadi A, Rosen J and Gogotsi Y 2021 *Science* **372** 1165
[20] Zhang T Z, Chang L B, Zhang X F, Wan H J, Liu N, Zhou L J and Xiao X 2022 *Nat. Commun.* **13** 6731
[21] Zhou C K, Wang D, Lagunas F, Atterberry B, Lei M, Hu H C, Zhou Z R, Filatov A S, Jiang D E, Rossini A J, Klie R F and Talapin D V 2023 *Nat. Chem.* **15** 1722
[22] Liu Y, Weiss N O, Duan X D, Cheng H C, Huang Y and Duan X F 2016 *Nat. Rev. Mater.* **1** 16042
[23] Novoselov K S, Mishchenko A, Carvalho A and Neto A H C 2016 *Science* **353** 512
[24] Cao Y, Fatemi V, Fang S, Watanabe K, Taniguchi T, Kaxiras E and Jarillo-Herrero P 2018 *Nature* **556** 43
[25] Cao Y, Fatemi V, Demir A, Fang S, Tomarken S L, Luo J Y, Sanchez-Yamagishi J D, Watanabe K, Taniguchi T, Kaxiras E, Ashoori R C and Jarillo-Herrero P 2018 *Nature* **556** 80
[26] Serlin M, Tschirhart C L, Polshyn H, Zhang Y, Zhu J, Watanabe K, Taniguchi T, Balents L and Young A F 2020 *Science* **367** 900
[27] Lu Z G, Han T H, Yao Y X, Reddy A P, Yang J X, Seo J, Watanabe K, Taniguchi T, Fu L and Ju L 2024 *Nature* **626** 759
[28] Kang K F, Shen B W, Qiu Y C, Zeng Y H, Xia Z C, Watanabe K, Taniguchi T, Shan J and Mak K F 2024 *Nature* **628** 522
[29] Sharpe A L, Fox E J, Barnard A W, Finney J, Watanabe K, Taniguchi T, Kastner M A and Goldhaber-Gordon D 2019 *Science* **365** 605
[30] Tran K, Moody G and Wu F C 2019 *Nature* **567** 71
[31] Wang X R, Yasuda K, Zhang Y, Liu S, Watanabe K, Taniguchi T, Hone J, Fu L and Jarillo-Herrero P 2022 *Nat. Nanotechnol.* **17** 367
[32] Regan E C, Wang D Q, Jin C H, Utama M I, Gao B N, Wei X, Zhao S H, Zhao W Y, Zhang Z C, Yumigeta K, Blei M, Carlstrom J D, Watanabe K, Taniguchi T, Tongay S, Crommie M, Zettl A and Wang F 2020 *Nature* **579** 359
[33] Nuckolls K P and Yazdani A 2024 *Nat. Rev. Mater.* **9** 460
[34] Sun L Z, Wang Z H and Wang Y C 2021 *Nat. Commun.* **12** 2391
[35] Bistritzer R and MacDonald A H 2011 *Proc. Natl. Acad. Sci. USA* **108** 12233
[36] Utama M I B, Koch R J, Lee K, Leconte N, Li H Y, Zhao S H, Jiang L L, Zhu J Y, Watanabe K, Taniguchi T, Ashby P D, Weber-Bargioni A, Zettl A, Jozwiak C, Jung J, Rotenberg E, Bostwick A and Wang F 2021 *Nat. Phys.* **17** 184

[37] Yang H, Liu L W, Yang H X, Zhang Y, Wu X, Huang Y, Gao H J and Wang Y L 2023 *Nano Res.* **16** 2579

[38] Yoo H, Engelke R, Carr S, Fang S A, Zhang K, Cazeaux P, Sung S H, Hoyden R, Tsen A W, Taniguchi T, Watanabe K, Yi G C, Kim M, Luskin M, Tadmor E B, Kaxiras E and Kim P 2019 *Nat. Mater.* **18** 448

[39] Yuk J M, Jeong H Y, Kim N Y, Park H J, Kim G, Shin H S, Ruoff R S, Lee J Y and Lee Z 2014 *Carbon* **80** 755

[40] Yasuda K, Wang X R, Watanabe K, Taniguchi T and Jarillo-Herrero P 2021 *Science* **372** 1458

[41] Huang D, Choi J, Shih C K and Li X Q 2022 *Nat. Nanotechnol.* **17** 227

[42] Yang W, Chen G R, Shi Z W, Liu C C, Zhang L C, Xie G B, Cheng M, Wang D M, Yang R, Shi D X, Watanabe K, Taniguchi T, Yao Y G, Zhang Y B and Zhang G Y 2013 *Nat. Mater.* **12** 792

[43] Bao Y, Shao J J, Xu H, Yan J X, Jing P T, Xu J L, Zhan D, Li B H, Liu K W, Liu L and Shen D Z 2024 *ACS Nano* **18** 27411

[44] Yuan Y L, Chu Y B, Hu C, Tian J P, Liu L, Wu F F, Ji Y R, Zhao J J, Huang Z H, Zan X Z, Du L J, Watanabe K, Taniguchi T, Shi D X, Shi Z W, Yang W and Zhang G Y 2023 *Chin. Phys. B* **32** 077304

[45] Cao Y, Rodan-Legrain D, Rubies-Bigorda O, Park J M, Watanabe K, Taniguchi T and Jarillo-Herrero P 2020 *Nature* **583** 215

[46] Chen S W, He M H, Zhang Y H, Hsieh V, Fei Z Y, Watanabe K, Taniguchi T, Cobden D H, Xu X D, Dean C R and Yankowitz M 2021 *Nat. Phys.* **17** 374

[47] Hao Z Y, Zimmerman A M, Ledwith P, Khalaf E, Najafabadi D H, Watanabe K, Taniguchi T, Vishwanath A and Kim P 2021 *Science* **371** 1133

[48] Zhang Y R, Polski R, Lewandowski C, Thomson A, Peng Y, Choi Y, Kim H, Watanabe K, Taniguchi T, Alicea J, von Oppen F, Refael G and Nadj-Perge S 2022 *Science* **377** 1538

[49] Yankowitz M, Xue J M, Cormode D, Sanchez-Yamagishi J D, Watanabe K, Taniguchi T, Jarillo-Herrero P, Jacquod P and LeRoy B J 2012 *Nat. Phys.* **8** 382

[50] Dean C R, Young A F, Meric I, Lee C, Wang L, Sorgenfrei S, Watanabe K, Taniguchi T, Kim P, Shepard K L and Hone J 2010 *Nat. Nanotechnol.* **5** 722

[51] Wang L, Meric I, Huang P Y, Gao Q, Gao Y, Tran H, Taniguchi T, Watanabe K, Campos L M, Muller D A, Guo J, Kim P, Hone J, Shepard K L and Dean C R 2013 *Science* **342** 614

[52] Shen C, Chu Y, Wu Q, Li N, Wang S, Zhao Y, Tang J, Liu J, Tian J, Watanabe K, Taniguchi T, Yang R, Meng Z Y, Shi D, Yazyev O V and Zhang G 2020 *Nat. Phys.* **16** 520

[53] Li E, Hu J X, Feng X M, Zhou Z S, An L H, Law K T, Wang N and Lin N 2021 *Nat. Commun.* **12** 5601

[54] Xu F, Sun Z, Jia T T, Liu C, Xu C, Li C S, Gu Y, Watanabe K, Taniguchi T, Tong B B, Jia J F, Shi Z W, Jiang S W, Zhang Y, Liu X X and Li T X 2023 *Phys. Rev. X* **13** 031037

[55] Yuan L, Zheng B Y, Kunstmann J, Brumme T, Kuc A B, Ma C, Deng S B, Blach D, Pan A L and Huang L B 2020 *Nat. Mater.* **19** 617

[56] Wang X, Zhu J Y, Seyler K L, Rivera P, Zheng H Y, Wang Y Q, He M H, Taniguchi T, Watanabe K, Yan J Q, Mandrus D G, Gamelin D R, Yao W and Xu X D 2021 *Nat. Nanotechnol.* **16** 1208

[57] Huang X Y, Han X, Dai Y Y, Xu X L, Yan J H, Huang M T, Ding P F, Zhang D C, Chen H, Laxmi V, Wu X, Liu L W, Wang Y L, Xu Y and Huang Y 2023 *J. Semicond.* **44** 011901

[58] Huang Y, Sutter E, Shi N N, Zheng J B, Yang T Z, Englund D, Gao H J and Sutter P 2015 *ACS Nano* **9** 10612

[59] Huang Y, Wang X, Zhang X, Chen X J, Li B W, Wang B, Huang M, Zhu C Y, Zhang X W, Bacsa W S, Ding F and Ruoff R S 2018 *Phys. Rev. Lett.* **120** 186104

[60] Liao M Z, Wei Z, Du L J, Wang Q Q, Tang J, Yu H, Wu F F, Zhao J J, Xu X Z, Han B, Liu K H, Gao P, Polcar T, Sun Z P, Shi D X, Yang R and Zhang G Y 2020 *Nat. Commun.* **11** 2153

[61] Wu K, Wang H, Yang M, Liu L, Sun Z Y, Hu G J, Song Y P, Han X, Guo J A, Wu K H, Feng B J, Shen C M, Huang Y, Shi Y G, Cheng Z G, Yang H T, Bao L H, Pantelides S T and Gao H J 2024 *Adv. Mater.* **36** 2313511

[62] Castellanos-Gomez A, Duan X F, Fei Z, Gutierrez H R, Huang Y, Huang X Y, Quereda J, Qian Q, Sutter E and Sutter P 2022 *Nat. Rev. Methods Primers* **2** 58

[63] Martins L G P, Song Y, Zeng T Y, Dresselhaus M S, Kong J and Araujo P T 2013 *Proc. Natl. Acad. Sci. USA* **110** 17762

[64] Quellmalz A, Wang X J, Sawallich S, Uzlu B, Otto M, Wagner S, Wang Z X, Prechtl M, Hartwig O, Luo S W, Duesberg G S, Lemme M C, Gylfason K B, Roxhed N, Stemme G and Niklaus F 2021 *Nat. Commun.* **12** 917

[65] Gao X, Zheng L M and Luo F 2022 *Nat. Commun.* **13** 5410

[66] Huang X L, Wan Z H, Yuan G W, Zhou Z J and Gao L B 2024 *J. Phys.: Condens. Matter* **36** 335304

[67] Lu Z Y, Chen Y, Dang W Q, Kong L A, Tao Q Y, Ma L K, Lu D L, Liu L T, Li W Y, Li Z W, Liu X, Wang Y L, Duan X D, Liao L and Liu Y 2023 *Nat. Commun.* **14** 2340

[68] Yuan G W, Liu W L, Huang X L, Wan Z H, Wang C, Yao B, Sun W J, Zheng H, Yang K H, Zhou Z J, Nie Y F, Xu J and Gao L B 2023 *Nat. Commun.* **14** 5457

[69] Gao L B, Ren W C, Xu H L, Jin L, Wang Z X, Ma T, Ma L P, Zhang Z Y, Fu Q, Peng L M, Bao X H and Cheng H M 2012 *Nat. Commun.* **3** 699

[70] Chen S S, Chen G and Zhao Y X 2024 *Adv. Mater.* **36** 2308950

[71] Hu Z N, Li F F and Wu H T 2023 *Adv. Mater.* **35** 2300621

[72] Wang M, Jang S K, Jang W J, Kim M, Park S Y, Kim S W, Kahng S J, Choi J Y, Ruoff R S, Song Y J and Lee S 2013 *Adv. Mater.* **25** 2746

[73] Shi Y M, Zhou W, Lu A Y, Fang W J, Lee Y H, Hsu A L, Kim S M, Kim K K, Yang H Y, Li L J, Idrobo J C and Kong J 2012 *Nano Lett.* **12** 2784

[74] Deng B, Wang B B, Li N, Li R T, Wang Y N, Tang J L, Fu Q, Tian Z, Gao P, Xue J M and Peng H L 2020 *ACS Nano* **14** 1656

[75] Liu S, He B Z, Yang W, Zhou X H, Xue X D, Liu M Y, Zhao Y, Wang X H, Si J, Wang F Y, Zhang Z Y, Peng L M and Yu G 2024 *Adv. Mater.* **36** 2312125

[76] Xu M Z, Ji H J, Zhang M W, Zheng L, Li W W, Luo L, Chen M D, Liu Z, Gan X T, Wang X W and Huang W 2024 *Adv. Mater.* **36** 2313638

[77] Li C, Xin R F, Jiao C Y, Zhang Z J, Qin J Z, Chu W L, Zhou X L, Li Z A, Wang Z H, Xia J and Zhou Y 2023 *J. Cent. South Univ.* **30** 3187

[78] Zhou J, Huang H J, Zhao Z H, Dou Z L, Zhou L, Zhang T T, Huang Z H, Feng Y B, Shi D X, Liu N, Yang J, Nie J, Wang Q Q, Dong J C, Liu Y Q, Dou R F and Xue Q K 2024 *Adv. Mater.* **36** 2408227

[79] Zhang X M, Nan H Y, Xiao S Q, Wan X, Gu X F, Du A J, Ni Z H and Ostrikov K 2019 *Nat. Commun.* **10** 598

[80] Peng G, Yang X, Wang S Y, Zhang J Y, Qi G J, Zhang S, Liu K, Zhu Z H, Li Z, Wang G, Zhu M J and Qin S Q 2020 *ACS Appl. Mater. Interfaces* **12** 23347

[81] Chang C, Zhang X W, Li W X, Guo Q L, Feng Z, Huang C, Ren Y L, Cai Y Y, Zhou X, Wang J H, Tang Z L, Ding F, Wei W Y, Liu K H and Xu X Z 2024 *Nat. Commun.* **15** 4130

[82] Gong Y J, Lin J H, Wang X L, Shi G, Lei S D, Lin Z, Zou X L, Ye G L, Vajtai R, Yakobson B I, Terrones H, Terrones M, Tay B K, Lou J, Pantelides S T, Liu Z, Zhou W and Ajayan P M 2014 *Nat. Mater.* **13** 1135

[83] Gao T, Song X J, Du H W, Nie Y F, Chen Y B, Ji Q Q, Sun J Y, Yang Y L, Zhang Y F and Liu Z F 2015 *Nat. Commun.* **6** 6835

[84] Liang J Y, Zhu X L, Chen M X, Duan X D, Li D and Pan A L 2022 *Acc. Mater. Res.* **3** 999

[85] Liu H W, Li D, Ma C, Zhang X H, Sun X X, Zhu C G, Zheng B Y, Zou Z X, Luo Z Y, Zhu X L, Wang X and Pan A L 2019 *Nano Energy* **59** 66

[86] Liu H W, Zhu X L, Sun X X, Zhu C G, Huang W, Zhang X H, Zheng B Y, Lou Z X, Luo Z Y, Wang X, Li D and Pan A L 2019 *ACS Nano* **13** 13573

[87] Zhang C, Zheng B Y, Wu G C, Liu X Y, Wu J X, Yao C D, Wang Y Z, Tang Z L, Chen Y, Fang L Z, Huang L Y, Li D, Li S M and Pan A L 2024 *Nano Res.* **17** 1856

[88] Gong Y J, Lei S D, Ye G L, Li B, He Y M, Keyshar K, Zhang X, Wang Q Z, Lou J, Liu Z, Vajtai R, Zhou W and Ajayan P M 2015 *Nano Lett.* **15** 6135

[89] Zhou Z J, Hou F C, Huang X L, Wang G, Fu Z H, Liu W L, Yuan G W, Xi X X, Xu J, Lin J H and Gao L B 2023 *Nature* **621** 499

[90] Tian F Y, Faizan M, He X, Sun Y H and Zhang L J 2024 *Chin. Phys. B* **33** 077403

[91] Zhang C H, Zhao S L, Jin C H, Koh A L, Zhou Y, Xu W G, Li Q C, Xiong Q H, Peng H L and Liu Z F 2015 *Nat. Commun.* **6** 6519

[92] Fu L, Sun Y Y, Wu N, Mendes R G, Chen L F, Xu Z, Zhang T, Rümmeli M H, Rellinghaus B, Pohl D, Zhuang L and Fu L 2016 *ACS Nano* **10** 2063

[93] Bierman M J, Lau Y K A, Kvit A V, Schmitt A L and Jin S 2008 *Science* **320** 1060

[94] Tay R Y, Park H J, Ling J J, Ng Z K, Jing L, Li H L, Zhu M M, Tsang S H, Lee Z and Teo E H T 2018 *Chem. Mater.* **30** 6858

[95] Zhao Y Z, Zhang C Y, Kohler D D, Scheeler J M, Wright J C, Voyles P M and Jin S 2020 *Science* **370** 442

[96] Zhang L M, Liu K H, Wong A B, Kim J, Hong X P, Liu C, Cao T, Louie S G, Wang F and Yang P D 2014 *Nano Lett.* **14** 6418

[97] Liu J Y, Huang Q Q, Qian Y Q, Huang Z G, Lai F C, Lin L M, Guo M Z, Zheng W F and Qu Y 2016 *Cryst. Growth Des.* **16** 2052

[98] Link R, Marcus G and Carroll D 2022 *Front. Mater.* **9** 963775

[99] Xia J, Zhu D D, Wang L, Huang B, Huang X and Meng X M 2015 *Adv. Funct. Mater.* **25** 4255

[100] Liu C, Li Z H and Qiao R X 2022 *Nat. Mater.* **21** 1263

[101] Li S S 2021 *Iscience* **24** 103229

[102] Li S S, Wang S F, Tang D M, Zhao W J, Xu H L, Chu L Q, Bando Y, Golberg D and Eda G 2015 *Appl. Mater. Today* **1** 60

[103] Carmalt C J, Parkin I P and Peters E S 2003 *Polyhedron* **22** 1499

[104] Li S S, Lin Y C and Zhao W 2018 *Nat. Mater.* **17** 535

[105] Kim M, Seo J, Kim J, Moon J S, Lee J, Kim J H, Kang J and Park H 2021 *ACS Nano* **15** 3038

[106] Shao G L, Xue X X, Zhou X L, Xu J, Jin Y Y, Qi S Y, Liu N, Duan H G, Wang S S, Li S S, Ouzounian M, Hu T S, Luo J, Liu S and Feng Y X 2019 *ACS Nano* **13** 8265

[107] Wang H, Huang X W and Lin J H 2017 *Nat. Commun.* **8** 394

[108] Fu Q D, Wang X W, Zhou J D, Xia J, Zeng Q S, Lv D H, Zhu C, Wang X L, Shen Y, Li X M, Hua Y N, Liu F C, Shen Z X, Jin C H and Liu Z 2018 *Chem. Mater.* **30** 4001

[109] Fortin-Deschênes M, Watanabe K, Taniguchi T and Xia F N 2024 *Nat. Mater.* **23** 339

[110] Shao G L, Xue X X, Liu X, Zhang D L, Jin Y Y, Wu Y W, You B Y, Lin Y C, Li S S, Suenaga K, Wang X, Pan A L, Li H M, Hong J H, Feng Y X and Liu S 2020 *Chem. Mater.* **32** 9721

[111] Zheng H H, Guo H L, Chen S L, Wu B, Li S F, He J, Liu Z W, Lu G, Duan X D, Pan A L and Liu Y P 2023 *Adv. Mater.* **35** 2210909

[112] Xu M Z, Ji H J, Zheng L, Li W W, Wang J, Wang H X, Luo L, Lu Q B, Gan X T, Liu Z, Wang X W and Huang W 2024 *Nat. Commun.* **15** 562

[113] Liu C F and Wang J 2022 *Chin. Phys. Lett.* **39** 077301

[114] Wang N, Jiang B B and Li M 2025 *Appl. Math. Lett.* **160** 109316

[115] Kezilebieke S, Huda N, Vano V, Aapro M, Ganguli S C, Silveira O J, Glodzik S, Foster A S, Ojanen T and Liljeroth P 2020 *Nature* **588** 424

[116] Zhao W M, Zhu L, Nie Z W, Li Q Y, Wang Q W, Dou L G, Hu J G, Xian L D, Meng S and Li S C 2022 *Nat. Mater.* **21** 284

[117] Pham T T, Vancsó P, Szendro M, Palotás K, Castelino R, Bouatou M, Chacon C, Henrard L, Lagoute J and Sporken R 2022 *npj 2D Mater. Appl.* **6** 48

[118] Kosiel K 2008 *Vacuum* **82** 951

[119] Choucair M, Thordarson P and Stride J A 2009 *Nat. Nanotechnol.* **4** 30

[120] Gong S, Zhao G Y, Zhang N Q and Sun K N 2019 *Chemelectrochem* **6** 3393

[121] Yu X B, Zhao G Y, Gong S, Liu C, Wu C L, Lyu P B, Maurin G and Zhang N Q 2020 *ACS Appl. Mater. Interfaces* **12** 24777

[122] Jiang C Y, Baggioli M and Jiang Q D 2024 *Phys. Rev. Lett.* **132** 166901

[123] Liao M Z, Nicolini P, Du L J, Yuan J H, Wang S P, Yu H, Tang J, Cheng P, Watanabe K, Taniguchi T, Gu L, Claerbout V E P, Silva A, Kramer D, Polcar T, Yang R, Shi D X and Zhang G Y 2022 *Nat. Mater.* **21** 47

[124] Liao M Z, Wu Z W, Du L J, Zhang T T, Wei Z, Zhu J Q, Yu H, Tang J, Gu L, Xing Y X, Yang R, Shi D X, Yao Y G and Zhang G Y 2018 *Nat. Commun.* **9** 4068

[125] Ribeiro-Palau R, Zhang C J, Watanabe K, Taniguchi T, Hone J and Dean C R 2018 *Science* **361** 690

[126] Hu C, Wu T Y, Huang X Y, Dong Y L, Chen J J, Zhang Z C, Lyu B S, Ma S Q, Watanabe K, Taniguchi T, Xie G B, Li X J, Liang Q and Shi Z W 2022 *Sci. Rep.* **12** 204

[127] Chen H, Zhang X L, Zhang Y Y, Wang D F, Bao D L, Que Y D, Xiao W D, Du S X, Ouyang M, Pantelides S T and Gao H J 2019 *Science* **365** 1036